The cross-talk between canonical and non-canonical Wnt-dependent pathways regulates P-glycoprotein expression in human blood-brain barrier cells.

UNIVERSITÀ DEGLI STUDI DI TORINO

The cross-talk between canonical and non canonical Wnt-dependent pathways regulates P-glycoprotein expression in human blood brain barrier cells

Martha L. Pinzón -Daza [1,2], PhD, Iris C. Salaroglio [1], MSc, Joanna Kopecka [1], PhD, Ruth Garzòn [2], PhD, Pierre-Olivier Couraud [3], PhD, Dario Ghigo [1,4], MD, Chiara Riganti [1,4], MD

[1] Department of Oncology, School of Medicine, University of Turin, via Santena 5/bis, 10126, Turin, Italy

[2] Unidad de Bioquímica, Facultad de Ciencias Naturales y Matemáticas, Universidad del Rosario, Quinta Mutis Carrera 24 #63C-69, Bogotá, Colombia

[3] Institut Cochin, Centre National de la Recherche Scientifique UMR 8104, Institut National de la Santé et de la Recherche Médicale (INSERM) U567, Université René Descartes, 22 rue Mechain, 75014, Paris, France

[4] Center for Experimental Research and Medical Studies, University of Turin, via Santena 5/bis, 10126, Turin, Italy

Correspondence: Prof. Dario Ghigo, Department of Oncology, University of Turin, via Santena 5/bis, 10126 Turin, Italy; phone: +390116705849; fax: +390116705845; email: dario.ghigo@unito.it

Funding sources

This work has been supported by grants from Compagnia di San Paolo, Italy (Neuroscience Program; grant 2008.1136), Italian Association for Cancer Research (AIRC; grant MFAG 11475), Italian

Ministry of University and Research (Future in Research FIRB 2012 Program; grant RBFR12SOQ1) to CR.

MLP-D and RG are recipients of a ERACOL Erasmus Mundus fellowship provided by EU. JK is recipient of a “Mario and Valeria Rindi” fellowship provided by Italian Foundation for Cancer Research (FIRC).

Disclosure/Conflict of Interest

The authors declare no conflict of interest.

Running title

Wnt controls P-glycoprotein in blood brain barrier

Abstract

In this work we investigate if and how transducers of the “canonical” Wnt pathway, i.e. Wnt/glycogen synthase kinase 3 (GSK3)/β-catenin, and transducers of the “non canonical” Wnt pathway, i.e. Wnt/RhoA/RhoA kinase, cooperate to control the expression of P-glycoprotein (Pgp) in blood brain barrier (BBB) cells.

By analyzing human primary brain microvascular endothelial cells constitutively activated for RhoA, silenced for RhoA or treated with the RhoA kinase inhibitor Y27632, we found that RhoA kinase phosphorylated and activated the protein tyrosine phosphatase 1B (PTP1B), which dephosphorylated tyrosine 216 of GSK3, decreasing the GSK3-mediated inhibition of β-catenin. By contrast, the inhibition of RhoA/RhoA kinase axis prevented the activation of PTP1B, enhanced the GSK3-induced phosphorylation and ubiquitination of β-catenin, reduced the β-catenin-driven transcription of Pgp. The RhoA kinase inhibition increased the delivery of Pgp substrates like doxorubicin across the BBB and improved the doxorubicin efficacy against glioblastoma cells co-cultured under a BBB monolayer.

Our data demonstrate that in human BBB cells the expression of Pgp is controlled by a cross-talk between canonical and non canonical Wnt pathways. The disruption of this cross-talk, e.g. by inhibiting RhoA kinase, down-regulates Pgp and increases the delivery of Pgp substrates across the BBB.

Keywords: blood brain barrier; β-catenin; glycogen synthase kinase 3; P-glycoprotein; RhoA kinase; Wnt.

Introduction

The blood brain barrier (BBB), a peculiar microvascular endothelium in the central nervous system, limits the delivery of drugs, xenobiotics and toxic catabolites into the brain parenchyma, owing to the absence of fenestrations, the abundance of tight junctions and adherens junctions, the presence of efflux transporters belonging to the ATP binding cassette (ABC) family.[1] P-glycoprotein (Pgp) is one of the ABC transporters present on the luminal side of BBB cells: it effluxes back into the bloodstream several chemotherapeutic drugs (e.g. anthracyclines, taxanes, Vinca alkaloids, epipodophyllotoxins, topotecan, methotrexate, imatinib, dasatinib, lapatinib, gefitinib, sorafenib, erlotinib), analgesics, anti-epileptics, anti-retrovirals, antibiotics.[1]

The Wnt signaling plays a central role in regulating the expression of Pgp in BBB cells [2,3] and relies on the simultaneous activation of different intracellular transducers. In the so-called "Wnt canonical pathway", the soluble Wnt proteins bind to the Frizzled receptor and the low-density-lipoprotein receptor related protein-5 and -6 (LRP5/LRP6) co-receptors, reduces the activity of glycogen synthase kinase 3 (GSK3), allowing the release of β-catenin from the cytosolic APC/axin complex and its translocation into the nucleus. Here β-catenin binds to the T-cell factor/lymphoid enhancer factor (TCF/LEF) and induces the transcription of target genes, such as *mdr1*, which encodes for Pgp.[4,5] We recently demonstrated that the disruption of the Wnt3 canonical pathway down-regulates the Pgp expression in human BBB cells.[6]

A plethora of intracellular transducers is involved in the so-called "non canonical Wnt pathways". By interacting with Frizzled, Wnt recruits Disheveled (Dvl), stimulates the small GTPases RhoA and Rac, activates RhoA kinase, mitogen activated protein (MAP) kinase kinases, MAP kinases, Jun N-terminal kinase.[4,7] By interacting with the co-receptors ROR2 and RYK, Wnt enhances the activity of phospholipase C, increases the intracellular calcium, activates protein kinase C (PKC) and calmodulin

kinases.[4] Wnt canonical and non canonical pathways are often reciprocally modulated, with either cooperative or antagonistic effects.[8,9]

The Wnt non canonical transducers RhoA and RhoA kinase regulate the integrity of tight junctions and the paracellular transport of substrates across BBB [10], as well as the activity of Pgp.[11] It is not known whether Wnt/RhoA/RhoA kinase pathway controls also the expression of Pgp.

Aim of this work is to investigate if there are cross-talk mechanisms between the Wnt/GSK3/β-catenin canonical pathway and the Wnt/RhoA/RhoA kinase non canonical pathway in human BBB cells, and how these cross-talks control the expression of Pgp and the delivery of Pgp substrates across BBB.

Materials and methods

Chemicals

The plasticware for cell cultures was from Falcon (Becton Dickinson, Franklin Lakes, NJ). WntA [2-amino-4-(3,4-(methylenedioxy)benzylamino)-6-(3-methoxyphenyl)pyrimidine] and Y27632 were purchased from Calbiochem (San Diego, CA). Human recombinant Dickkopf-1 (Dkk-1) was from R&D Systems (Minneapolis, MN). Rho activator II, a synthetic derivative of cytotoxic necrotizing factor from *E. coli* which maintains RhoA constitutively activated[12], was from Cytoskeleton Inc. (Denver, CO). The electrophoresis reagents were obtained from Bio-Rad Laboratories (Hercules, CA). The protein content of cell lysates was assessed with the BCA kit from Sigma Chemicals Co (St. Louis, MO). When not otherwise specified, all the other reagents were purchased from Sigma Chemicals Co.

Cells

The hCMEC/D3 cells, a primary human brain microvascular endothelial cell line that retains the BBB characteristics *in vitro* [13], were seeded at 50 000/cm² density, grown for 7 days up to confluence in Petri dishes or Transwell devices (0.4 μm diameter pore-size, Corning Life Sciences, Chorges, France), and cultured as previously reported. [13]

The primary human glioblastoma cells (CV17, 01010627, Nov3) were obtained from surgical samples of patients from the Neuro-Biooncology Center, Vercelli, Italy and the DIBIT San Raffaele Scientific Institute, Milan, Italy. The tumor diagnosis was performed according to WHO guidelines. The U87-MG cell line was purchased from ATCC (Manassas, VA). The cells were cultured as already reported.[6] The experimental protocols were approved by the Bioethics Committee ("Comitato di Bioetica d'Ateneo"), University of Turin, Italy.

In co-culture experiments, 500 000 (for intracellular doxorubicin accumulation, cytotoxicity assays and cell cycle analysis) or 1 000 (for proliferation assay) glioblastoma cells were added in the lower chamber of Transwell devices, 4 days after seeding hCMEC/D3 cells in the Transwell insert. After 3 days of co-culture the medium of the upper chamber was replaced with fresh medium or with medium containing Y27632 and doxorubicin, alone or in combination, as detailed in the Figure legends.

Western blot analysis

The cells were rinsed with lysis buffer (50 mmol/L Tris, 10 mmol/L EDTA, 1% v/v Triton-X100), supplemented with the protease inhibitor cocktail set III (80 μmol/L aprotinin, 5 mmol/L bestatin, 1.5 mmol/L leupeptin, 1 mmol/L pepstatin; Calbiochem), 2 mmol/L phenylmethylsulfonyl fluoride and 1 mmol/L $NaVO_4$, then sonicated and centrifuged at 13 000 x g for 10 min at 4°C. 20 μg protein extracts were subjected to SDS-PAGE and probed with the following antibodies: anti-GSK3 (BD Biosciences, Franklin Lakes, NJ); anti-phospho(Tyr216)GSK3 (BD Biosciences); anti-β-catenin (BD Biosciences);

anti-phospho(Ser33/Ser37/Thr41)β-catenin (Cell Signaling Technology Inc., Danvers, MA); anti-claudin 3 (Invitrogen Life Technologies, Monza, Italy); anti-claudin 5 (Invitrogen Life Technologies); anti-occludin (Invitrogen Life Technologies); anti-zonula occludens-1 (ZO-1; Invitrogen Life Technologies); anti-protein tyrosine phosphatase 1B (PTP1B; Abcam, Cambridge, UK); anti-phospho(Ser50)PTP1B (Abcam); anti-Pgp (clone C219, Calbiochem); anti-multidrug resistance related protein 1 (MRP1; Abcam); anti-breast cancer resistance protein (BCRP; Santa Cruz Biotechnology Inc., Santa Cruz, CA); anti-caspase-3 (C33, GeneTex, Hsinhu City, Taiwan); anti-β-tubulin (Santa Cruz Biotechnology Inc.), followed by a peroxidase-conjugated secondary antibody (Bio-Rad). The membranes were washed with Tris-buffered saline-Tween 0.1% v/v, and the proteins were detected by enhanced chemiluminescence (Bio-Rad).

To assess the presence of ubiquitinated β-catenin, 100 μg of proteins from whole cell extracts were immunoprecipitated with the anti-β-catenin antibody, using the PureProteome protein A and protein G Magnetic Beads (Millipore, Billerica, MA). The immunoprecipitated proteins were separated by SDS-PAGE and probed with an anti-ubiquitin antibody (Enzo Life Science, Farmingdale, NY), followed by a peroxidase-conjugated secondary antibody.

10 μg of nuclear extracts, obtained with the Nuclear Extraction Kit (Active Motif, Rixensart, Belgium), were subjected to Western blot analysis using an anti-β-catenin antibody. To check the equal control loading in nuclear fractions, the samples were probed with an anti-TATA-binding protein (TBP/TFIID) antibody (Santa Cruz Biotechnology Inc.). To exclude any cytosolic contamination of nuclear extracts, we verified that β-tubulin was undetectable in nuclear samples (not shown).

The densitometric analysis of Western blots was performed with the ImageJ software (http://rsb.info.nih.gov/ij/) and expressed as arbitrary units, where “1 unit” is the mean band density of untreated hCMEC/D3 cells.

Chromatin Immunoprecipitation (ChIP)

The ChIP experiments were performed using the Magna ChIP™ A/G Chromatin Immunoprecipitation Kit (Millipore). The samples were immunoprecipitated with 5 μg of an anti-β-catenin antibody or with no antibody. The immunoprecipitated DNA was washed and eluted twice with 100 μL of elution buffer (0.1 mol/L $NaHCO_3$, 1% w/v SDS), the cross-linking was reversed by incubating the samples at 65°C for 6 h. The samples were then treated with 1 μL proteinase K for 1 h at 55°C. The DNA was eluted in 50 μL of H_2O and analyzed by quantitative real time-PCR (qRT-PCR). The putative β-catenin site on *mdr1* promoter was validated by the MatInspector software (http://www.genomatix.de/); the primers sequences were: 5'-CGATCCGCCTAAGAACAAAG-3'; 5'-AGCACAAATTGAAGGAAGGAG-3'. As negative control, the immunoprecipitated samples were subjected to PCR with primers matching a region 10,000 bp upstream the *mdr1* promoter, using the following primers: 5'-GTGGTGCCTGAGGAAGAGAG-3'; 5'-GCAACAAGTAGGCACAAGCA-3'. The qRT-PCR was carried out using an IQ™ SYBR Green Supermix (Bio-Rad); the data were analyzed with a Bio-Rad Software Gene Expression Quantitation (Bio-Rad).

qRT-PCR

Total RNA was extracted and reverse-transcribed using the QuantiTect Reverse Transcription Kit (Qiagen, Hilden, Germany). The qRT-PCR was performed with the IQ™ SYBR Green Supermix (Bio-Rad). The same cDNA preparation was used to quantify the genes of interest and the housekeeping gene *β-actin*. The primer sequences, designed with the Primer3 software (http://frodo.wi.mit.edu/primer3), were: for *mdr1*: 5'-TGCTGGAGCGGTTCTACG-3'; 5'-ATAGGCAATGTTCTCAGCAATG-3'; for *β-actin*: 5'- GCTATCCAGGCTGTGCTATC-3'; 5'-TGTCACGCACGATTTCC-3'. The relative quantification was performed by comparing each PCR

product with the housekeeping PCR product, using the Bio-Rad Software Gene Expression Quantitation (Bio-Rad).

RhoA and RhoA kinase activity

To evaluate the RhoA activity, the RhoA-GTP-bound fraction, taken as an index of monomeric G-proteins activation [11], was measured using the G-LISA™ RhoA Activation Assay Biochem Kit (Cytoskeleton Inc.), according to the manufacturer's instructions. The absorbance was read at 450 nm, using a Packard EL340 microplate reader (Bio-Tek Instruments, Winooski, VT). For each set of experiments, a titration curve was prepared, using serial dilutions of the Rho-GTP positive control of the kit. The data were expressed as U absorbance/mg cell proteins. The RhoA kinase activity was measured using the CycLex Rho Kinase Assay Kit (CycLex Co., Nagano, Japan), following the manufacturer's instructions. For each set of experiments, a titration curve was set, using serial dilutions of recombinant RhoA kinase (MBL Inc., Woburn, MA). The data were expressed as U absorbance/mg cell proteins.

RhoA siRNA transfection

200 000 cells were transfected with 400 nmol/L of 20-25 nucleotide non targeting scrambled siRNAs (Control siRNA-A, Santa Cruz Biotechnology Inc.) or specific RhoA siRNAs (Santa Cruz Biotechnology Inc.), as reported previously.[14] To verify the silencing efficacy, 48 h after the transfection the cells were lysed and checked for the expression of RhoA by Western blotting, using an anti-RhoA antibody (Santa Cruz Biotechnology Inc.).

PTP1B activity

To measure the activity of endogenous PTB1B in cell lysates, the PTP1B Inhibitor Screening Assay kit (Abcam) was used. Cells untreated or treated with RhoA activator II, Y27632 or both, were washed

twice in ice-cold PBS, detached by trypsin/EDTA, rinsed with 0.5 mL of PTP1B assay buffer provided by the kit and sonicated. 200 μL of cell lysate, each containing 100 μg proteins, were transferred into a 96-wells plate, in the presence of 100 μmol/L PTP1B substrate from the kit. The plates were incubated for 30 min at 37°C, then 100 μL of the Red Assay reagent of the kit were added for 20 min. The absorbance at 620 nm was read using a Packard EL340 microplate reader.

The activity of purified PTP1B was measured in a cell-free system: 5 U of human recombinant PTP1B protein (Abcam), diluted in 100 μL of reaction buffer (10 mmol/L Tris/HCl, 50 mmol/L NaCl, 2 mmol/L dithiothreitol, 1 mmol/L $MnCl_2$; pH 7.5), were incubated for 10 min at 37°C, with 10 μg of a recombinant peptide from human GSK3 containing phosphorylated tyrosine 216 (Abcam). To test if RhoA kinase affects the dephosphorylation of GSK3 by PTP1B, in a parallel set of experiments PTP1B protein was pre-incubated for 30 min at 37°C with 10 U of human recombinant RhoA kinase (MBL Inc.), diluted in 100 μL of the Rho Kinase buffer (from CycLex Rho Kinase Assay Kit) containing 25 mmol/L ATP. When indicated, 10 μmol/L of the RhoA kinase inhibitor Y27632 was added. After this pre-incubation step, a 10 μL aliquot from each sample was removed and used to measure the phosphorylation of PTP1B on serine 50 by Western blot analysis. The remaining sample was incubated for 10 min at 37°C with the phospho(Tyr 216)-GSK3 peptide, as reported above. In all samples the reaction was stopped by adding 100 μL of the Red Assay reagent from the PTP1B Inhibitor Screening Assay kit; the absorbance at 620 nm was read after 20 min. For each set of experiments, a titration curve was prepared, using serial dilutions of the phosphate standard from the PTP1B Inhibitor Screening Assay kit. Data were expressed as nmol phosphate/mL. The activity of endogenous PTP1B was then expressed as percentage of the activity of PTP1B of each sample versus the activity of PTP1B measured in untreated cells. The activity of purified PTP1B was expressed as percentage of the activity

of PTP1B measured after the pre-incubation step with RhoA kinase versus the activity of PTP1B measured without the pre-incubation step with RhoA kinase.

Permeability assays across BBB

The permeability to dextran-fluorescein isothiocyanate (FITC; molecular weight 70 kDa), [^{14}C]-sucrose (molecular weight: 342.30 Da; 589 mCi/mmol; PerkinElmer, Waltham, MA), [^{14}C]-inulin (molecular weight range: 5.0-5.5 kDa; 10 mCi/mmol; PerkinElmer), sodium fluorescein (molecular weight: 376.27 Da) was taken as a parameter of tight junction integrity [11,15] and measured as previously reported.[6,16]

To measure the permeability coefficient of doxorubicin across the BBB monolayer, wild-type or RhoA-silenced hCMEC/D3 cells were grown for 7 days up to confluence in 6-multiwell Transwell devices, and treated as reported under the Results section. 5 μmol/L doxorubicin was added in the upper Transwell chamber for 3 h, then the medium in the lower chamber was collected and the amount of doxorubicin was measured fluorimetrically, using an LS-5 spectrofluorimeter (PerkinElmer). The excitation and emission wavelengths were 475 nm and 553 nm, respectively. The fluorescence was converted in nmol doxorubicin/cm^2, using a calibration curve prepared previously. The permeability coefficients were calculated as reported earlier.[17]

Intratumor doxorubicin accumulation in co-culture models

After 3 days of co-culture, doxorubicin (5 μmol/L for 3 h) or Y27632 (10 μmol/L for 3 h) followed by doxorubicin (5 μmol/L for 3 h) were added to the upper chamber of a Transwell insert containing an hCMEC/D3 cell monolayer. Then glioblastoma cells were collected from the lower chamber, rinsed with PBS, re-suspended in 0.5 mL ethanol/HCl 0.3 N (1:1 v/v) and sonicated. A 50 μL aliquot was used to measure the protein content; the remaining sample was used to quantify fluorimetrically the

intracellular doxorubicin content, as described above. The results were expressed as nmol doxorubicin/mg cell proteins.

For fluorescence microscope analysis, the glioblastoma cells in the lower chamber were seeded on sterile glass coverslips and treated as reported above. At the end of the incubation period, the cells were rinsed with PBS, fixed in 4% w/v paraformaldehyde for 15 min, washed three times with PBS and incubated with 4',6-diamidino-2-phenylindole dihydrochloride (DAPI) for 3 min at room temperature in the dark. The cells were washed three times with PBS and once with water, then the slides were mounted with 4 μL of Gel Mount Aqueous Mounting and examined with a Leica DC100 fluorescence microscope (Leica Microsystems GmbH, Wetzlar, Germany). For each experimental point, a minimum of 5 microscopic fields were examined.

Cytotoxicity, cell cycle analysis and cell proliferation of glioblastoma cells in co-culture models

For cytotoxicity, apoptosis and cell cycle analysis, after 3 days of co-culture, doxorubicin (5 μmol/L for 24 h) or Y27632 (10 μmol/L for 3 h) followed by doxorubicin (5 μmol/L for 24 h) were added to the upper chamber of Transwell inserts containing an hCMEC/D3 cell monolayer.

The release of lactate dehydrogenase (LDH) in the supernatant of glioblastoma cells, used as an index of cell damage and necrosis, was measured spectrophotometrically as described earlier.[18] The apoptosis of glioblastoma cells was assessed by analyzing the cleavage of caspase-3 by Western blotting, as described above. For cell cycle distribution, the glioblastoma cells were washed twice with fresh PBS, incubated in 0.5 mL of ice-cold 70% v/v ethanol for 15 min, then centrifuged at 1 200 x g for 5 min at 4°C and rinsed with 0.3 mL of citrate buffer (50 mM Na_2HPO_4, 25 mM sodium citrate, 1% v/v Triton X-100), containing 10 μg/mL propidium iodide and 1 mg/mL RNAse (from bovine pancreas). After a 15 min incubation in the dark, the intracellular fluorescence was detected by a FACSCalibur flow

cytometer (Becton Dickinson). For each analysis, 10 000 events were collected and analyzed by the Cell Quest software (Becton Dickinson).

To monitor the long-term cell proliferation, 1 000 glioblastoma cells were seeded in the lower chamber of Transwell, containing confluent hCMEC/D3 cells in the insert. This time was considered “day 0” in the proliferation assay. After 3 days of co-culture, the upper chamber of the Transwell insert was filled with fresh medium or medium containing 10 μmol/L Y27632 for 3 h, 5 μmol/L doxorubicin for 24 h, 10 μmol/L Y27632 for 3 h followed by 5 μmol/L doxorubicin for 24 h. The treatments were repeated every 7 days, for 4 weeks. At day 7, 14, 21, 28 the glioblastoma cells were collected, transferred into a 96-wells plate, fixed with 4% w/v paraformaldehyde and stained with 0.5% w/v crystal violet solution for 10 min at room temperature. The plate was washed three times in water, then 100 μL of 0.1 mmol/L sodium citrate in 50 % v/v ethanol was added to each well and the absorbance was read at 570 nm. The absorbance units were converted into the number of cells, according to a titration curve obtained with serial cell dilutions of each cell line. To check that the hCMEC/D3 cells retained BBB properties, the permeability to dextran and inulin was measured weekly in a parallel set of Transwell. No significant changes in the permeability coefficients were detected during the whole experiment (not shown).

Pgp ATPase assay

The rate of ATP hydrolysis was measured spectrophotometrically on Pgp immunoprecipitated from the membrane of hCMEC/D3 cells as described previously.[11]

Statistical analysis

All data in text and figures are provided as means ± SD. The results were analyzed by a one-way Analysis of Variance (ANOVA). A $p < 0.05$ was considered significant.

Results

Wnt controls the GSK3/β-catenin and RhoA/RhoA kinase activities in human BBB cells

The hCMEC/D3 cells exhibited a GSK3 constitutively phosphorylated on tyrosine 216, i.e. activated, and a β-catenin constitutively phosphorylated on serine 33, serine 37 and threonine 41 (Figure 1A), i.e. primed for ubiquitination. Notwithstanding, we detected in the untreated hCMEC/D3 cells a basal amount of β-catenin translocated into the nucleus (Figure 1B) and bound to the promoter of *mdr1* gene (Figure 1C), which encodes for Pgp. In line with previous findings obtained on hCMEC/D3 cells and primary human brain microvascular endothelial cells[6], the Wnt activator WntA decreased the phosphorylation/activation of GSK3, strongly reduced the phosphorylation of β-catenin (Figure. 1A), increased the nuclear translocation and the binding of β-catenin to the *mdr1* promoter (Figure 1B-C); the Wnt inhibitor Dkk-1 produced opposite effects (Figure 1A-C). In keeping with these results, WntA increased and Dkk-1 decreased the mRNA level of *mdr1* in hCMEC/D3 cells (Figure 1D). In parallel, Wnt modulated the activity of RhoA and RhoA kinase: as shown in Figure 1E, WntA increased and Dkk-1 decreased the GTP binding to RhoA and the activity of RhoA kinase. These data suggest that both Wnt/GSK3 canonical pathway and Wnt/RhoA/RhoA kinase non canonical pathway are active in the hCMEC/D3 cells and vary their activity in response to Wnt activators and inhibitors at the same time.

RhoA modulates the GSK3/β-catenin-driven transcription of Pgp in human BBB cells

To investigate whether the activity of non canonical Wnt/RhoA/RhoA kinase pathway controls the activity of canonical Wnt/GSK3 pathway in hCMEC/D3 cells, we constitutively activated RhoA with

the RhoA activator II [12] (Figure 2A) and silenced RhoA (Figure 2B), respectively. The cells with active RhoA showed a reduced phosphorylation of GSK3 and β-catenin (Figure 2C), and an increased β-catenin nuclear translocation (Figure 2D). By contrast, the RhoA-silenced cells exhibited a higher amount of phosphorylated GSK3 and β-catenin (Figure 2C), and a reduced β-catenin nuclear translocation (Figure 2D). These data suggest that the activity of the Wnt non canonical transducer RhoA controls the activation of the Wnt canonical transducers GSK3/β-catenin in our model.

Of note for the aim of this work, the RhoA activation increased, while the RhoA silencing decreased the binding of β-catenin to *mdr1* promoter (Figure 2E) and the levels of *mdr1* mRNA (Figure 2F) in the hCMEC/D3 cells. The increase of *mdr1* expression induced by WntA or RhoA activator II was not paralleled by an increase in permeability to small molecules, such as sucrose and sodium fluorescein (Supplementary Figure 1), thus ruling out a Wnt- or RhoA-mediated increase of the monolayer passive permeability.

The RhoA kinase inhibition reduces the Pgp transcription in BBB cells, by inhibiting the PTP1B activity and increasing the GSK3-mediated phosphorylation and ubiquitination of β-catenin

Since in hCMEC/D3 cells Wnt controls the activity of RhoA and its downstream effector RhoA kinase (Figure 1E), we next investigated whether RhoA kinase mediated the cross-talk between the Wnt/GSK3 canonical pathway and the Wnt/RhoA non canonical pathway. Time-dependence experiments with the RhoA kinase inhibitor Y27632 showed that at 10 μmol/L this compound effectively inhibited the RhoA kinase activity at each time point considered (Supplementary Figure 2A) and decreased the β-catenin nuclear translocation at the time points from 3 to 24 h (Supplementary Figure 2B). After 3 h, when the reduction of RhoA kinase activity and β-catenin was maximal, Y27632 did not change the expression of claudin-3, claudin-5, occludin, ZO-1 (Supplementary Figure 2C) and did not alter the permeability

coefficient of dextran, inulin and sucrose (Supplementary Figure 2D), suggesting that the RhoA kinase inhibition did not affect the integrity of tight junctions and the paracellular transport processes. In the light of these results, Y27632 was used at 10 μmol/L for 3 h in all the following experiments: in these conditions, Y27632 increased the phosphorylation of GSK3 and β-catenin (Figure 3A) and reduced the β-catenin nuclear translocation (Figure 3B), also in the presence of a constitutively activated RhoA (Figure 3A-B).

The tyrosine phosphatase PTP1B reduces the activity of GSK3 by dephosphorylating tyrosine 216, which is critical for the GSK3 activity.[19] PTP1B is in its turn activated by the phosphorylation on serine 50, operated by serine/threonine kinases.[20] We thus wondered whether RhoA kinase may modulate the GSK3 phosphorylation via PTP1B.

PTP1B was basally phosphorylated on serine 50 in the hCMEC/D3 cells (Figure 3C). Interestingly, the cells with activated RhoA had increased levels of phospho(Ser50)PTP1B, which was strongly reduced in cells treated with the RhoA kinase inhibitor Y27632. The latter also abolished the phosphorylation of PTP1B induced by active RhoA (Figure 3C). The endogenous activity of PTP1B was significantly increased in cells with activated RhoA and significantly decreased in Y27632-treated cells (Figure 3D). To test whether RhoA kinase, by phosphorylating PTP1B on serine 50, may decrease the phosphorylation of GSK3 on tyrosine 216, we set up a cell-free system and measured the activity of recombinant PTP1B protein, using as a substrate a synthetic peptide derived from GSK3, containing the phosphorylated tyrosine 216 (Figure 3E-F). PTP1B, when pre-incubated with the recombinant RhoA kinase in this cell-free system, was phosphorylated on serine 50, an effect that was prevented by Y27632 (Figure 3E). In keeping with this observation, the pre-incubation with RhoA kinase increased

the PTP1B-mediated dephosphorylation of the recombinant phospho(Tyr 216)GSK3 peptide; such a dephosphorylation was significantly reduced by the RhoA kinase inhibitor Y27632 (Figure 3F).

These data suggest that RhoA kinase activates PTP1B, promotes the tyrosine dephosphorylation of GSK3 and its inhibition, whereas the RhoA kinase inhibition produces opposite effects.

Since an active GSK3 promotes the phosphorylation of β-catenin, priming it for the subsequent ubiquitination and proteasomal degradation [4,5], we next measured the β-catenin ubiquitination in the presence of RhoA/RhoA kinase activators or inhibitors. The untreated hCMEC/D3 cells showed a basal level of β-catenin ubiquitination (Figure 4A), which was in line with the basal phosphorylation of the protein on serine 33, serine 37 and threonine 41 (Figure 1A). The ubiquitination of β-catenin was reduced in cells with active RhoA and increased by the RhoA silencing or the RhoA kinase inhibitor Y27632 (Figure 4A). These data suggest that an active RhoA kinase prevents the ubiquitination of β-catenin and highlight the possibility to regulate the transcription of β-catenin-target genes by modulating the RhoA kinase activity. As the silencing of RhoA did (Figure. 2E-F), also Y27632 decreased the binding of β-catenin to the *mdr1* promoter (Figure 4B) and the levels of *mdr1* mRNA (Figure 4C). Both RhoA silencing and RhoA kinase inhibition reduced the Pgp protein levels, whereas RhoA increased them; by contrast, these treatments did not change the amount of MRP1 and BCRP, two other ABC transporters present on the luminal side of BBB cells[1] (Figure 4D).

To verify whether the inhibition of RhoA and RhoA kinase increases the delivery of Pgp substrates across the BBB, we used doxorubicin [21], which exhibited a low permeability across the hCMEC/D3 cell monolayer (Figure 4E), due to the high level of Pgp on the luminal side of these cells.[22] The doxorubicin permeability was further decreased by active RhoA, but it was increased by RhoA silencing or Y27632 (Figure 4E). The latter, which counteracted the effect of RhoA activator II on β-

catenin ubiquitination (Figure 4A), also prevented the effects of RhoA activation on β-catenin binding to *mdr1* promoter (Figure 4B), *mdr1* transcription (Figure 4C), Pgp protein levels (Figure 4D) and doxorubicin permeability (Figure 4E).

The inhibition of RhoA kinase increases the doxorubicin delivery and cytotoxicity in human glioblastoma cells co-cultured with BBB cells

Since the inhibition of RhoA kinase increased the doxorubicin permeability across the hCMEC/D3 monolayer, we wondered whether priming the BBB cells with Y27632 improves the delivery of doxorubicin to glioblastoma cells grown under the BBB monolayer.

The doxorubicin accumulation within glioblastoma cells (CV17, 01010627, Nov3 and U87-MG) co-cultured with hCMEC/D3 cells was low, as evaluated by fluorimetric assays (Figure 5A) and fluorescence microscope analysis (Figure 5B). The pre-treatment of the hCMEC/D3 cells with Y27632 significantly increased the doxorubicin retention within glioblastoma cells (Figure 5A-B). Doxorubicin alone did not produce significant cell damages in terms of release of LDH in the extracellular medium of glioblastoma cells (Figure 5C), and induced weak signs of apoptosis, as suggested by the low level of cleaved caspase-3 (Figure 5D). When effective, the drug is expected to induce a G2/M-phase arrest, which was not observed in the 01010627 glioblastoma cells co-cultured under the hCMEC/D3 monolayer exposed to doxorubicin alone (Figure 5E). The exposure to Y27632 followed by doxorubicin strongly increased the release of LDH (Figure 5C), the cleavage of caspase-3 (Figure 5D), the percentage of cells arrested in G2/M phase (Figure 5E). In parallel such combination increased the amount of cells in pre-G1 phase, an index of apoptotic cells, and decreased the number of cells in S phase (Figure 5E). Of note, used at 10 µmol/L for 3 h, Y27632 alone was not cytotoxic for glioblastoma cells (Figure 5C-E). The repeated administration of Y27632 or doxorubicin as single

agents on the luminal side of the hCMEC/D3 monolayer did not reduce the proliferation of 01010627 glioblastoma cells growing under this model of BBB (Figure 5F); only the pre-treatment of hCMEC/D3 cells with Y27632 followed by doxorubicin significantly decreased the long-term proliferation of tumor cells (Figure 5F).

Interestingly, the pre-treatment with Y27632 produced the same effects of verapamil, a strong inhibitor of Pgp activity in the hCMEC/D3 cells (Supplementary Figure 3A); when co-incubated with doxorubicin, verapamil increased the drug permeability across the BBB monolayer (Supplementary Figure 3B) and its accumulation in co-cultured glioblastoma cells (Supplementary Figure 3C), as well as LDH release (Supplementary Figure 3D), caspase-3 activation (Supplementary Figure 3E), G2/M-arrest (Supplementary Figure 3F) in glioblastoma cells.

Discussion

In this work we demonstrate that the expression of Pgp in human BBB cells is controlled by a cross-talk between the Wnt/GSK3 canonical pathway and the Wnt/RhoA/RhoA kinase non canonical pathway. The activation of Wnt/GSK3/β-catenin axis is known to increase the expression of Pgp in hCMEC/D3 cells.[2,3,6] The activation of RhoA and RhoA kinase is known to enhance the Pgp activity in BBB cells.[11] It is not known: 1) whether the Wnt/RhoA/RhoA kinase axis controls also the Pgp expression; 2) whether the canonical and non canonical Wnt pathways cooperate in regulating the Pgp levels in BBB cells.

We observed that the Wnt activation increases at the same time the activity of GSK3 and the activity of RhoA/RhoA kinase in hCMEC/D3 cells, while the Wnt inhibition reduces them. The positive

cooperation between Wnt/GSK3 and Wnt/RhoA/RhoA kinase axis, which we detected in BBB cells, has been described in pulmonary aortic endothelial cells: here the bone morphogenetic protein 2 increases the activity of GSK3/β-catenin axis and at the same time recruits the Wnt-downstream effector Dvl, which activates RhoA.[23] Since WntA activates Dvl, and Dkk-1 inhibits it in most mammalian cells [4], it is likely that also in our model the changes in RhoA/RhoA kinase activity in response to WntA and Dkk-1 were due to changes in Dvl activity.

It has not been clarified however whether the canonical Wnt pathway controls the activity of the non canonical Wnt pathways or *vice versa*. In gastric cancer cells, the activation of RhoA in response to Wnt5a is dependent on the activation of the PI3K/Akt/GSK3 axis.[24] Our results demonstrated that an active RhoA decreases the activity of GSK3, prevents the GSK3-mediated phosphorylation of β-catenin, favors its nuclear translocation and the subsequent transcription of Pgp, whereas the RhoA silencing produces opposite effects. We therefore hypothesize that the RhoA activity controls the GSK3/β-catenin axis in hCMEC/D3 cells. This hypothesis is in contrast with results obtained in murine cerebrovascular endothelial cells, where the activation of RhoA promotes the phosphorylation of β-catenin and reduces its transcriptional activity.[9] Since murine and human brain microvascular cells have often striking differences in the expression and activity of Pgp [25], it is not surprising that they also differ in the upstream pathways controlling Pgp expression. For instance, the mechanism by which RhoA modulates GSK3 activity is quite different in murine and human cerebrovascular endothelial cells: in murine cells, RhoA controls the GSK3 activity in a PTEN- and PKCδ-dependent way and changes the phosphorylation of GSK3 on serine 9.[9] This phosphorylation has inhibitory effects on the enzymatic activity of GSK3.[26] We cannot exclude that the RhoA activity may change the phosphorylation on serine 9 of GSK3 also in human hCMEC/D3 cells; on the other hand, we observed that in our model the activation of RhoA decreases - and the silencing of RhoA increases - the

phosphorylation of GSK3 on tyrosine 216, which is a pro-activating phosphorylation.[26] When phosphorylated on tyrosine 216, GSK3 induces β-catenin phosphorylation and degradation. To our knowledge, this is the first work showing that RhoA activity modulates the phosphorylation on tyrosine 216 of GSK3.

We next looked for putative downstream effectors of RhoA responsible for this effect. We focused on RhoA kinase, whose activity followed the same trend of RhoA activity in response to WntA and Dkk-1 in hCMEC/D3 cells. Interestingly, the inhibition of RhoA kinase by Y27632 quickly decreased the nuclear translocation of β-catenin, with a maximal efficacy after 3 h. At longer time points, nuclear β-catenin progressively re-accumulated in the nucleus, although it remained lower than in untreated cells: this may be due to the short half-life (i.e. less than 12 h) of β-catenin[27], which produces a fast re-synthesis of new β-catenin ready to translocate into the nucleus. After 3 h, Y27632 effectively increased the phosphorylation on tyrosine 216 of GSK3 and the subsequent GSK3-induced phosphorylation of β-catenin; by acting downstream RhoA, Y27632 was effective even in cells with a constitutively activated RhoA. These data suggest that RhoA kinase likely controls the GSK3 activity by activating a tyrosine phosphatase, which recognizes GSK3 as substrate. PTP1B, which is activated by the phosphorylation on serine 50 [20], is one of these phosphatases.[19] Our results in hCMEC/D3 cells and in a cell-free system demonstrate that the RhoA kinase phosphorylates PTPB1 on serine 50, promoting the dephosphorylation of GSK3 on tyrosine 216, an event that was fully abrogated by Y27632. These data suggest that the RhoA kinase, by activating PTPB1, inhibits the GSK3 activity, prevents the ubiquitination of β-catenin, and allows its nuclear translocation and transcriptional activity. Our results also explain previous observations, showing that Wnt3 stimulates the transcription of β-catenin-target genes and RhoA-target genes, with a putative RhoA kinase-dependent mechanism.[8]

Some β-catenin-target genes encode for proteins of adherens junctions and tight junctions; therefore, changes in RhoA/RhoA kinase activity may lead to the loss of BBB integrity.[10] In our experimental conditions no changes occurred in the protein expression and functionality of tight junctions in the hCMEC/D3 cells treated with Y27632. By contrast, Y27632 was sufficient to reduce the β-catenin-driven transcription of Pgp. Since different promoters have different sensitivity to the binding of β-catenin/TCF complex, we might speculate that the promoter of Pgp is more sensitive than the promoter of other genes to the variations of β-catenin/TCF binding.

Working at proper concentrations and incubation times, the RhoA kinase inhibitor increased the delivery of doxorubicin, a Pgp substrate with a very low permeability across the BBB.[13] Fasudil, the clinically prescribed analog of Y27632, is used to prevent vasospasms after subarachnoid hemorrhage[28], to improve tissue perfusion during cerebral ischemia[29], to prevent the progression of cerebral aneurisms.[30] Our work suggests that Fasudil might be used to improve the delivery of Pgp substrates through the BBB.

In the case of doxorubicin, a drug which is highly effective against glioblastoma cells *in vitro* [31] and ineffective in the presence of a competent BBB [6], the pre-treatment of hCMEC/D3 cells with Y27632 fully restored the doxorubicin delivery and cytotoxicity in glioblastoma cells. Repeated pulses of Y27632 followed by doxorubicin confirmed that this approach effectively reduced the long-term proliferation of glioblastoma cells grown under a BBB monolayer. On the other hand, Pgp is not the only transporter present on the luminal side of BBB that can efflux doxorubicin: also MRP1 and BCRP, which are detectable in the hCMEC/D3 cells[11], meet these requisites[1], but their expression did not change in cells with constitutively active RhoA, silenced for RhoA or treated with Y27632. We thus hypothesize that the changes in doxorubicin delivery following RhoA activation or inhibition were consequent to the expression change of Pgp in hCMEC/D3 cells. To further quantify the contribution of

this transporter in doxorubicin permeability, we treated the hCMEC/D3 cells with the Pgp inhibitor verapamil, which produced the same effects – in terms of doxorubicin delivery and toxicity in glioblastoma cells – of Y27632. These results indirectly suggest that Pgp plays a major role in limiting doxorubicin delivery in the central nervous system. Although Pgp tightly cooperates with BCRP in controlling the delivery of several drugs across the BBB[32], doxorubicin has high affinity for Pgp, which represents the main transporter of this drug in BBB cells[33].

The down-regulation of the canonical Wnt/GSK3/β-catenin pathway is known to reduce the Pgp expression and to induce chemosensitization in colon[34] and glioblastoma[17] tumor stem cells, neuroblastoma[35], chronic myeloid leukemia[36], cholangiocarcinoma.[37] Also the inhibition of the non canonical Wnt3/RhoA/RhoA kinase pathway chemosensitizes multiple myeloma cells to doxorubicin.[38] We might speculate that the same cross-talk between canonical and non canonical Wnt pathways, observed in BBB cells, cooperates in regulating the Pgp expression also in cancer cells, and may represent a critical target of therapeutic intervention for Pgp-rich tumors.

We suggest that the expression of Pgp is controlled by a cross-talk between canonical and non canonical Wnt pathways in human BBB cells. A crucial regulator of this cross-talk is RhoA kinase, which inhibits the GSK3-induced phosphorylation of β-catenin by activating PTP1B. Targeted therapies against RhoA/RhoA kinase can disrupt the cross-talk and down-regulate the Pgp expression (Figure 6). Improving the BBB permeability of anticancer drugs that are effluxed by Pgp thus enhancing their delivery to brain tumors is still an unsolved challenge.[39] Moreover, the high expression of Pgp on BBB cells decreases not only the delivery of chemotherapeutic agents, but also the passage of drugs used to treat infective diseases, neurodegenerative diseases and epilepsy.[40] By unveiling a new mechanism that regulates Pgp expression in the BBB cells, our work may pave the way to pre-clinical investigations using RhoA kinase inhibitors as adjuvant tools in these central nervous system diseases.

Disclosure/Conflict of Interest

The authors declare no conflict of interest.

Acknowledgements

We thanks Mr. Costanzo Costamagna, Dept. of Oncology, University of Turin, for the technical assistance. We are grateful to Prof. Davide Schiffer (Neuro-Biooncology Center, Vercelli, Italy) and Dr. Rossella Galli (DIBIT, San Raffaele Scientific Institute, Milan, Italy) for providing the primary glioblastoma samples.

Supplementary information is available at the Journal of Cerebral Blood Flow & Metabolism website – www.nature.com/jcbfm

References

1. Agarwal S, Sane R, Oberoi R, Ohlfest JR, Elmquist WF. Delivery of molecularly targeted therapy to malignant glioma, a disease of the whole brain. *Expert Rev Mol Med* 2011; 13: e17.

2. Lim JC, Kania KD, Wijesuriya H, Chawla S, Sethi JK, Pulaski L, *et al*. Activation of β-catenin signalling by GSK-3 inhibition increases p-glycoprotein expression in brain endothelial cells. *J Neurochem* 2008; 106: 1855-1865.

3. Kania KD, Wijesuriya HC, Hladky SB, Barrand MA. Beta amyloid effects on expression of multidrug efflux transporters in brain endothelial cells. *Brain Res* 2011; 1418: 1-11.

4. Katoh M, Katoh M. WNT signalling pathway and stem cells signaling network. *Clin Cancer Res* 2007; 13: 4042-4045.

5. MacDonald BT, Tamai K, He X. Wnt/β-catenin signaling: components, mechanisms, and diseases. *Dev Cell* 2009; 17: 9-26.

6. Riganti C, Salaroglio IC, Pinzòn-Daza ML, Caldera V, Campia I, Kopecka J, *et al*. Temozolomide down-regulates P-glycoprotein in human blood-brain barrier cells by disrupting Wnt3-signalling. *Cell Mol Life Sci* 2014; 71: 499-516.

7. Tsuji T, Ohta Y, Kanno Y, Hirose K, Ohashi K, Mizuno K. Involvement of p114-RhoGEF and Lfc in Wnt-3a- and dishevelled-induced RhoA activation and neurite retraction in N1E-115 mouse neuroblastoma cells. *Mol Biol Cell* 2010; 21: 3590-3600.

8. Rossol-Allison J, Stemmle LN, Swenson-Fields KI, Kelly P, Fields PE, McCall SJ, *et al*. Rho GTPase activity modulates Wnt3a/beta-catenin signaling. *Cell Signal* 2009; 21: 1559-1568.

9. Chang CC, Lee PS, Chou Y, Hwang LL, Juan SH. Mediating effects of aryl-hydrocarbon receptor and RhoA in altering brain vascular integrity: the therapeutic potential of statins. *Am J Pathol* 2012; 181: 211-221.

10. Allen C, Srivastava K, Bayraktutan U. Small GTPase RhoA and its effector rho kinase mediate oxygen glucose deprivation-evoked in vitro cerebral barrier dysfunction. *Stroke* 2010; 41: 2056-2063.

11. Pinzón-Daza ML, Garzón R, Couraud PO, Romero IA, Weksler B, Ghigo D, *et al*. The association of statins plus LDL receptor-targeted liposome-encapsulated doxorubicin increases the *in vitro* drug delivery across blood-brain barrier cells. *Brit J Pharmacol* 2012; 167: 1431-1447.

12. Flatau G, Lemichez E, Gauthier M, Chardin P, Paris S, Fiorentini C, *et al*. Toxin-induced activation of the G protein p21 Rho by deamidation of glutamine. *Nature* 1997; 387: 729-733.

13. Weksler BB, Subileau EA, Perrière N, Charneau P, Holloway K, Leveque M, *et al*. Blood-brain barrier-specific properties of a human adult brain endothelial cell line. *FASEB J* 2005; 19: 1872-1894.

14. Doublier S, Riganti C, Voena C, Costamagna C, Aldieri E, Pescarmona G, *et al*. RhoA silencing reverts the resistance to doxorubicin in human colon cancer cells. *Mol Cancer Res* 2008; 6: 1607-1620.

15. Monnaert V, Betbeder D, Fenart L, Bricout H, Lenfant AM, Landry C, *et al*. Effects of γ- and hydroxypropyl- γ -cyclodextrins on the transport of doxorubicin across an in vitro model of blood-brain barrier. *J Pharmacol Exp Ther* 2004; 311: 1115-1120.

16. Eigenmann DE, Xue G, Kim KS, Moses AV, Hamburger M, Oufir M. Comparative study of four immortalized human brain capillary endothelial cell lines, hCMEC/D3, hBMEC, TY10, and BB19, and optimization of culture conditions, for an in vitro blood-brain barrier model for drug permeability studies. *Fluids Barriers CNS* 2013; 10: e33.

17. Siflinger-Birnboim A, Del Vecchio PJ, Cooper JA, Blumenstock FA, Shepard JM, Malik AB. Molecular sieving characteristics of the cultured endothelial monolayer. *J Cell Physiol* 1987; 132: 111-117.

18. Riganti C, Salaroglio IC, Caldera V, Campia I, Kopecka J, Mellai M, *et al*. Temozolomide down-regulates P-glycoprotein expression in glioblastoma stem cells by interfering with the Wnt3a/GSK3/β-catenin pathway. *Neuro-Oncol* 2013; 15: 1502-1517.

19. Mobasher MA, González-Rodriguez A, Santamaría B, Ramos S, Martín MÁ, Goya L, *et al*. Protein tyrosine phosphatase 1B modulates GSK3β/Nrf2 and IGFIR signaling pathways in acetaminophen-induced hepatotoxicity. *Cell Death Dis* 2003; 4: e626.

20. Moeslein FM, Myers MP, Landreth GE. The CLK family kinases, CLK1 and CLK2, phosphorylate and activate the tyrosine phosphatase, PTP-1B. *J Biol Chem* 1999; 274: 26697-26704.

21. Gottesman MM, Fojo T, Bates SE. Multidrug resistance in cancer: role of ATP-dependent transporters. *Nat Rev Cancer* 2002; 2: 48-58.

22. Tai LM, Loughlin AJ, Male DK, Romero IA. P-glycoprotein and breast cancer resistance protein restrict apical-to-basolateral permeability of human brain endothelium to amyloid-β. *J Cereb Blood Flow Metab* 2009; 29: 1079-1083.

23. de Jesus Perez VA, Alastalo TP, Wu JC, Axelrod JD, Cooke JP, Amieva M, *et al*. Bone morphogenetic protein 2 induces pulmonary angiogenesis via Wnt-beta-catenin and Wnt-RhoA-Rac1 pathways. *J Cell Biol* 2009; 184: 83-99.

24. Liu J, Zhang Y, Xu R, Du J, Hu Z, Yang L, *et al*. PI3K/Akt-dependent phosphorylation of GSK3β and activation of RhoA regulate Wnt5a-induced gastric cancer cell migration. *Cell Signal* 2013; 25: 447-456.

25. Uchida Y, Ohtsuki S, Katsukura Y, Ikeda C, Suzuki T, Kamiie J, *et al*. Quantitative targeted absolute proteomics of human blood-brain barrier transporters and receptors. *J Neurochem* 2011; 117: 333-345.

26. Jope RS, Johnson GV. The glamour and gloom of glycogen synthase kinase-3. *Trends Biochem Sci* 2004; 29: 95-102.

27. Bareiss S, Kim K, Lu Q. Delta-catenin/NPRAP: A new member of the glycogen synthase kinase-3beta signaling complex that promotes beta-catenin turnover in neurons. *J Neurosci Res* 2010; 88: 2350-2363.

28. Zoerle T, Ilodigwe DC, Wan H, Lakovic K, Sabri M, Ai J, *et al*. Pharmacologic reduction of angiographic vasospasm in experimental subarachnoid hemorrhage: systematic review and meta-analysis. *J Cereb Blood Flow Metab* 2012; 32: 1645-1658.

29. Shin HK, Huang PL, Ayata C. Rho-kinase inhibition improves ischemic perfusion deficit in hyperlipidemic mice. *J Cereb Blood Flow Metab* 2014; 34: 284-287.

30. Eldawoody H, Shimizu H, Kimura N, Saito A, Nakayama T, Takahashi A, *et al*. Fasudil, a Rho-kinase inhibitor, attenuates induction and progression of cerebral aneurysms: experimental study in rats using vascular corrosion casts. *Neurosci Lett* 2010; 470: 76-80.

31. Hau P, Fabel K, Baumgart U, Rummele P, Grauer O, Bock A, *et al*. Pegylated liposomal doxorubicin-efficacy in patients with recurrent high-grade glioma. *Cancer* 2004; 100: 1199-1207.

32. Agarwal S, Hartz AM, Elmquist WF, Bauer B. Breast cancer resistance protein and P-glycoprotein in brain cancer: two gatekeepers team up. *Curr Pharm Des* 2011; 17: 2793-2802.

33. Qu Q, Chu JW, Sharom FJ. Transition state P-glycoprotein binds drugs and modulators with unchanged affinity, suggesting a concerted transport mechanism. *Biochemistry* 2003; 42: 1345-1353.

34. Chikazawa N, Tanaka H, Tasaka T, Nakamura M, Tanaka M, Onishi H, *et al*. Inhibition of Wnt signaling pathway decreases chemotherapy-resistant side-population colon cancer cells. *Anticancer Res* 2010; 30: 2041-2048.

35. Flahaut M, Meier R, Coulon A, Nardou KA, Niggli FK, Martinet D, *et al*. The Wnt receptor FZD1 mediates chemoresistance in neuroblastoma through activation of the Wnt/beta-catenin pathway. *Oncogene* 2009; 28: 2245-2256.

36. Corrêa S, Binato R, Du Rocher B, Castelo-Branco MT, Pizzatti L, Abdelhay E. Wnt/β-catenin pathway regulates ABCB1 transcription in chronic myeloid leukemia. *BMC Cancer* 2012; 12: e303.

37. Shen DY, Zhang W, Zeng X, Liu CQ. Inhibition of Wnt/β-catenin signaling downregulates P-glycoprotein and reverses multi-drug resistance of cholangiocarcinoma. *Cancer Sci* 2013; 104: 1303-1308.

38. Kobune M, Chiba H, Kato J, Kato K, Nakamura K, Kawano Y, *et al*. Wnt3/RhoA/ROCK signaling pathway is involved in adhesion-mediated drug resistance of multiple myeloma in an autocrine mechanism. *Mol Cancer Ther* 2007; 6: 1774-1784.

39. Serwer LP, James CD. Challenges in drug delivery to tumors of the central nervous system: an overview of pharmacological and surgical considerations. *Adv Drug Deliv Rev* 2012; 64: 590-597.

40. Pinzón-Daza ML, Campia I, Kopecka J, Garzón R, Ghigo D, Riganti C. Nanoparticle- and liposome-carried drugs: new strategies for active targeting and drug delivery across blood-brain barrier. *Curr Drug Metab* 2013; 14: 625-640.

Titles and legends to figures

Figure 1. Wnt controls the β-catenin induced transcription of Pgp and RhoA activity in human BBB cells

The hCMEC/D3 cells were grown in fresh medium (*ctrl*), with the Wnt activator 2-amino-4-(3,4-(methylenedioxy)benzylamino)-6-(3-methoxyphenyl)pyrimidine (*WntA*; 20 μmol/L for 24 h) or the Wnt inhibitor Dkk-1 protein (*Dkk*; 1 μg/mL for 24 h) **A.** Western blot analysis of phospho(Tyr216)GSK3 (*pGSK3*), GSK3, phospho(Ser33/Ser37/Thr41)β-catenin (*pcat*), β-catenin (*cat*) in whole cell lysates. The β-tubulin expression was used as a control of equal protein loading. The figure is representative of 3 experiments with similar results. The band density ratio between each protein and β-tubulin was expressed as arbitrary units. Versus *ctrl* cells: * $p < 0.02$. **B**. Nuclear extracts were analyzed for the amount of β-catenin (*nucl cat*). The expression of TBP was used as a control of equal protein loading. The figure is representative of 3 experiments with similar results. The band density ratio between each protein and TBP was expressed as arbitrary units. Versus *ctrl* cells: * $p < 0.02$. **C.** ChIP assay. The genomic DNA was extracted, immunoprecipitated with an anti-β-catenin antibody and analyzed by qRT-PCR, using primers for the β-catenin binding site on *mdr1* promoter (*open bars*) or for an upstream region (*black bars*), chosen as a negative control. Results are presented as means ± SD (n = 4). Versus *ctrl*: * $p < 0.05$. **D.** The *mdr1* expression was detected by qRT-PCR. Data are presented as means $\pm$ SD (n = 4). Versus *ctrl*: * $p < 0.02$. **E.** RhoA/RhoA kinase activity. The samples were subjected to ELISA assays to measure the amount of RhoA-GTP (*open bars*) and the activity of RhoA kinase (*black bars*). Data are presented as means $\pm$ SD (n = 4). Versus *ctrl*: * $p < 0.05$.

Figure 2. The RhoA activity controls the GSK3/β-catenin-driven transcription of Pgp in human BBB cells

A. The hCMEC/D3 cells were grown in fresh medium in the absence (*ctrl*) or in the presence of the RhoA activator II (*RhoAc*; 5 µg/mL for 3 h), then the activity of RhoA was measured by an ELISA assay. Data are presented as means ± SD (n = 4). Versus *ctrl*: * $p < 0.005$. **B.** The cells were cultured for 48 h with fresh medium (*ctrl*), treated with a non targeting scrambled siRNA (*scr*) or a RhoA-targeting specific siRNA pool (*siRhoA*). The expression of RhoA was measured in whole cell lysates by Western blotting. The β-tubulin expression was used as a control of equal protein loading. The figure is representative of 3 experiments with similar results. The band density ratio between each protein and β-tubulin was expressed as arbitrary units. Versus *ctrl* cells: * $p < 0.005$. **C.** Western blot analysis of phospho(Tyr216)GSK3 (*pGSK3*), GSK3, phospho(Ser33/Ser37/Thr41)β-catenin (*pcat*), β-catenin (*cat*) in whole cell lysates of hCMEC/D3 cells treated as described in **A-B**. The β-tubulin expression was used as a control of equal protein loading. The figure is representative of 3 experiments with similar results. The band density ratio between each protein and β-tubulin was expressed as arbitrary units. Versus *ctrl* cells: * $p < 0.05$. **D.** Nuclear extracts from cells treated as described in **A-B** were analyzed for the amount of β-catenin (*nucl cat*). The expression of TBP was used as a control of equal protein loading. The band density ratio between each protein and TBP was expressed as arbitrary units. Versus *ctrl* cells: * $p < 0.005$. **E.** Cells were cultured as reported in **A-B.** After 3 h (for the RhoA activator II-treated cells) or 48 h (for the scrambled- and RhoA-targeting siRNA-treated cells), the genomic DNA was extracted, immunoprecipitated with an anti-β-catenin antibody and analyzed by qRT-PCR, using primers for the β-catenin binding site on the *mdr1* promoter (*open bars*) or for an upstream region (*black bars*), chosen as a negative control. The *ctrl* bars in the figure correspond to the DNA extracted after 48 h from hCMEC/D3 cells; the results were superimposable for the DNA extracted after 3 h (not shown in the figure). Results are expressed as means ± SD (n = 4). Versus *ctrl*: * $p < 0.01$. **F.** The cells were treated as detailed in **A-B**. After 3 h (for the RhoA activator II-treated cells) or 48 h (for the

scrambled- and RhoA-targeting siRNA-treated cells), the *mdr1* expression was detected by qRT-PCR. Data are presented as means ± SD (n = 4). Versus *ctrl*: * $p < 0.005$.

Figure 3. The RhoA kinase inhibition increases the activation of GSK3, by decreasing the activity of PTP1B in human BBB cells

The hCMEC/D3 cells were grown in fresh medium (*ctrl*) or in medium containing the RhoA activator II (*RhoAc*; 5 µg/mL for 3 h) or the RhoA kinase inhibitor Y27632 (*Y276*; 10 µmol/L for 3 h), alone or co-incubated. **A.** Western blot analysis of phospho(Tyr216)GSK3 (*pGSK3*), GSK3, phospho(Ser33/Ser37/Thr41)β-catenin (*pcat*), β-catenin (*cat*) in whole cell lysates. The β-tubulin expression was used as a control of equal protein loading. The figure is representative of 3 experiments with similar results. The band density ratio between each protein and β-tubulin was expressed as arbitrary units. Versus *ctrl* cells: * $p < 0.05$; versus *RhoAc* alone: ° $p < 0.001$. **B**. The nuclear extracts were analyzed for the amount of β-catenin (*nucl cat*). The expression of TBP was used as a control of equal protein loading. The band density ratio between each protein and TBP was expressed as arbitrary units. Versus *ctrl* cells: * $p < 0.002$; versus *RhoAc* alone: ° $p < 0.001$. **C**. Western blot analysis of phospho(Ser50)PTP1B (*pPTP1B*) and PTP1B. The β-tubulin expression was used as a control of equal protein loading. The figure is representative of 3 experiments with similar results. The band density ratio between each protein and β-tubulin was expressed as arbitrary units. Versus *ctrl* cells: * $p < 0.005$; versus *RhoAc* alone: ° $p < 0.001$. **D.** The activity of endogenous PTP1B was measured in cell lysates, as reported under Materials and methods. Data are presented as means ± SD (n = 3). Versus *ctrl*: * $p < 0.002$; versus *RhoAc* alone: ° $p < 0.001$. **E.** *In vitro* phosphorylation of PTP1B in the presence of RhoA kinase and Y27632. 5 U of human recombinant PTP1B were incubated in the absence (-) or in the presence of 10 U of human recombinant RhoA kinase (RhoAK), alone or in the presence of the RhoA kinase inhibitor Y27632 (*Y276*; 10 µmol/L) for 30 min at 37°C, in a reaction buffer containing 25

mmol/L ATP. At the end of this incubation time, samples were resolved by SDS-PAGE and probed with anti-phospho(Ser50)PTP1B (*pPTP1B*) or anti-PTP1B antibodies. The figure is representative of 3 experiments with similar results. **F.** The activity of purified PTP1B was measured in a cell-free system, using a recombinant phospho(Tyr 216)GSK3 peptide as substrate. When indicated, 10 U of RhoA kinase (*RhoAK*), alone or in the presence of Y27632 (*Y276*; 10 μmol/L), were added in the reaction mix 30 min before adding the phospho(Tyr 216)GSK3 peptide. Suramin (*sur*; 10 μmol/L), a known inhibitor of PTP1B, was added together with the phospho(Tyr 216)GSK3 peptide, as internal control. Data are presented as means ± SD (n = 3). Versus PTP1B alone (-): * $p < 0.002$; versus *RhoAK*: ° $p < 0.001$.

Figure 4. The RhoA kinase inhibition enhances the ubiquitination of β-catenin, down-regulates the β-catenin-induced transcription of Pgp and increases the doxorubicin permeability in human BBB cells

The hCMEC/D3 cells were grown in fresh medium (*ctrl*), or in medium containing the RhoA activator II (*RhoAc*; 5 μg/mL for 3 h) or the RhoA kinase inhibitor Y27632 (*Y276*; 10 μmol/L for 3 h), alone or co-incubated. When indicated, the cells were treated with a non targeting scrambled siRNA or a RhoA-targeting specific siRNA (*siRhoA*) for 48 h (panel **A**) or 72 h (panels **D**-**E**). **A.** Whole cell lysates were immunoprecipitated (*IP*) with an anti-β-catenin antibody, then immunoblotted (*IB*) with an anti-mono/polyubiquitin antibody or with an anti-β-catenin antibody. Cells treated with non targeting scrambled siRNA had the same level of ubiquitination than untreated (*ctrl*) cells (not shown).The figure is representative of 3 experiments with similar results. *no Ab*: samples immunoprecipitated without anti-β-catenin antibody. *MW*: molecular weight markers. The 92 kDa band corresponding to the native β-catenin protein is indicated by the arrow. **B.** Chromatin immunoprecipitation assay. The genomic DNA was extracted, immunoprecipitated with an anti-β-catenin antibody and analyzed by qRT-PCR,

using primers for the β-catenin binding site on the *mdr1* promoter (*open bars*) or for an upstream region (*black bars*), chosen as a negative control. Results are expressed as means ± SD (n = 4). Versus *ctrl*: * $p < 0.05$; versus *RhoAc*: ° $p < 0.01$. **C.** The *mdr1* expression was detected by qRT-PCR. Data are presented as means ± SD (n = 4). Versus *ctrl*: * $p < 0.005$; versus *RhoAc*: ° $p < 0.001$. **D.** Western blot analysis of Pgp, MRP1 and BCRP in the whole cell lysates of hCMEC/D3 cells treated as described above. The β-tubulin expression was used as a control of equal protein loading. The figure is representative of 3 experiments with similar results. The band density ratio between each protein and β-tubulin was expressed as arbitrary units. Versus *ctrl* cells: * $p < 0.02$; versus *RhoAc*: ° $p< 0.005$. **E.** Doxorubicin permeability. The cells were grown for 7 days up to confluence in Transwell inserts and incubated as reported above. At the end of the incubation period, doxorubicin (5 μmol/L) was added in the upper chamber. After 3 h the amount of drug recovered from the lower chamber was measured fluorimetrically. The permeability coefficient was calculated as reported under Materials and methods. In cells treated with the non targeting scrambled siRNA the permeability coefficient was 0.0018 ± 0.0002 (not significant versus *ctrl* cells). Measurements were performed in duplicate and data are presented as means ± SD (n = 3). Versus *ctrl*: * $p < 0.05$; versus *RhoAc*: ° $p< 0.02$.

Figure 5. The RhoA kinase inhibitor Y27632 increases the doxorubicin delivery and cytotoxicity in glioblastoma cells co-cultured with BBB cells

The hCMEC/D3 cells were grown for 7 days up to confluence in Transwell inserts; CV17, 01010627, Nov3 and U87-MG cells were seeded at day 4 in the lower chamber. After 3 days of co-culture, the supernatant in the upper chamber was replaced with fresh medium without (- or *ctrl*) or with Y27632 (*Y276*; 10 μmol/L for 3 h). After this incubation time, doxorubicin (*dox*; 5 μmol/L) was added in the upper chamber for 3 h (panels **A-B**) or 24 h (panels **C-F**), then the following investigations were

performed. **A**. Fluorimetric quantification of intracellular doxorubicin in glioblastoma cells. Data are presented as means ± SD (n = 4). Versus untreated (-) cells: * $p < 0.001$. **B**. The 01010627 cells were seeded on sterile glass coverslips, treated as reported above, then stained with DAPI and analyzed by fluorescence microscopy to detect the intracellular accumulation of doxorubicin. Magnification: 63 x objective (1.4 numerical aperture); 10 x ocular lens. The micrographs are representative of 3 experiments with similar results. Bar: 20 μm. **C**. The glioblastoma cells were checked spectrophotometrically for the extracellular release of LDH activity. Data are presented as means ± SD (n= 4). Versus untreated (-) cells: * $p < 0.001$. **D.** The whole cell lysates from 01010627 cells were resolved by SDS-PAGE and immunoblotted with an anti-caspase 3 antibody (recognizing both pro-caspase and cleaved active caspase). The β-tubulin expression was used as a control of equal protein loading. The figure is representative of 3 experiments with similar results. **E.** Cell cycle analysis. The distribution of the 01010627 cells in sub-G1, G0/G1, S, G2/M phase was analyzed by flow cytometry, as detailed under Materials and methods. Data are presented as means ± SD (n=4). Versus *ctrl*: * $p < 0.005$. **F.** After 3 days of co-culture between hCMEC/D3 and 01010627 cells, the medium of the upper chamber was replaced with fresh medium (*open circles*) or medium containing Y27632 (*Y276*; 10 μmol/L for 3 h, *solid circles*), doxorubicin (*dox*; 5 μmol/L for 24 h, *open squares*), Y27632 (*Y276*; 10 μmol/L for 3 h) followed by doxorubicin (*doxo*; 5 μmol/L for 24 h, *solid squares*). Drug treatments were repeated every 7 days, as reported in the Materials and methods section. The proliferation of glioblastoma cells was monitored weekly by crystal violet staining. Measurements were performed in triplicate and data are presented as means ± SD (n= 4). Versus *ctrl*: * $p < 0.001$.

Figure 6. Cross-talk between Wnt/GSK3 pathway and Wnt/RhoA/RhoA kinase pathway and effects on Pgp expression in human BBB cells

A. The Wnt activators (e.g. WntA) reduce the GSK3-mediated phosphorylation and ubiquitination of β-catenin, decreasing its proteasomal degradation. In these conditions, β-catenin is released from the APC/axin complex, translocates into the nucleus and activates the transcription of *mdr1* gene, which encodes for Pgp. The RhoA activation reduces as well the activity of GSK3: the active RhoA increases the activity of RhoA kinase, which induces the phosphorylation on serine 50 of PTP1B. After this phosphorylation, PTP1B dephosphorylates GSK3 on tyrosine 216 and inactivates it. Overall, the activation of the RhoA/RhoA kinase axis contributes to the transcription of β-catenin target genes, like *mdr1*. **B.** The Wnt inhibitors (e.g. Dkk-1) increase the GSK3-mediated phosphorylation and ubiquitination of β-catenin, priming it for the proteasomal degradation. The inhibition of RhoA (e.g. by RhoA siRNA) or RhoA kinase (e.g. by Y27632) increases the GSK3 activity, by reducing the RhoA kinase-mediated phosphorylation of PTP1B on serine 50 and preventing the dephosphorylation of GSK3 on tyrosine 216. As a result, the nuclear translocation of β-catenin and its transcriptional activity are reduced, whereas the ubiquitination and proteasomal degradation of β-catenin are increased. These data lead to hypothesize the existence of a cross-talk between the Wnt/GSK3 canonical pathway and the Wnt/RhoA/RhoA kinase non canonical pathway in human BBB cells. Friz: Frizzled; LRP5/6: low density lipoprotein receptor-related protein 5/6; RhoAc: RhoA activator II; APC: adenomatous polyposis coli; Pi: phosphate; Pi(Y): phosphotyrosine; RhoAK: RhoA kinase; Uq: ubiquitin. Continuous arrows indicate activated pathways; dotted arrows indicate inhibited pathways.

Figure 1

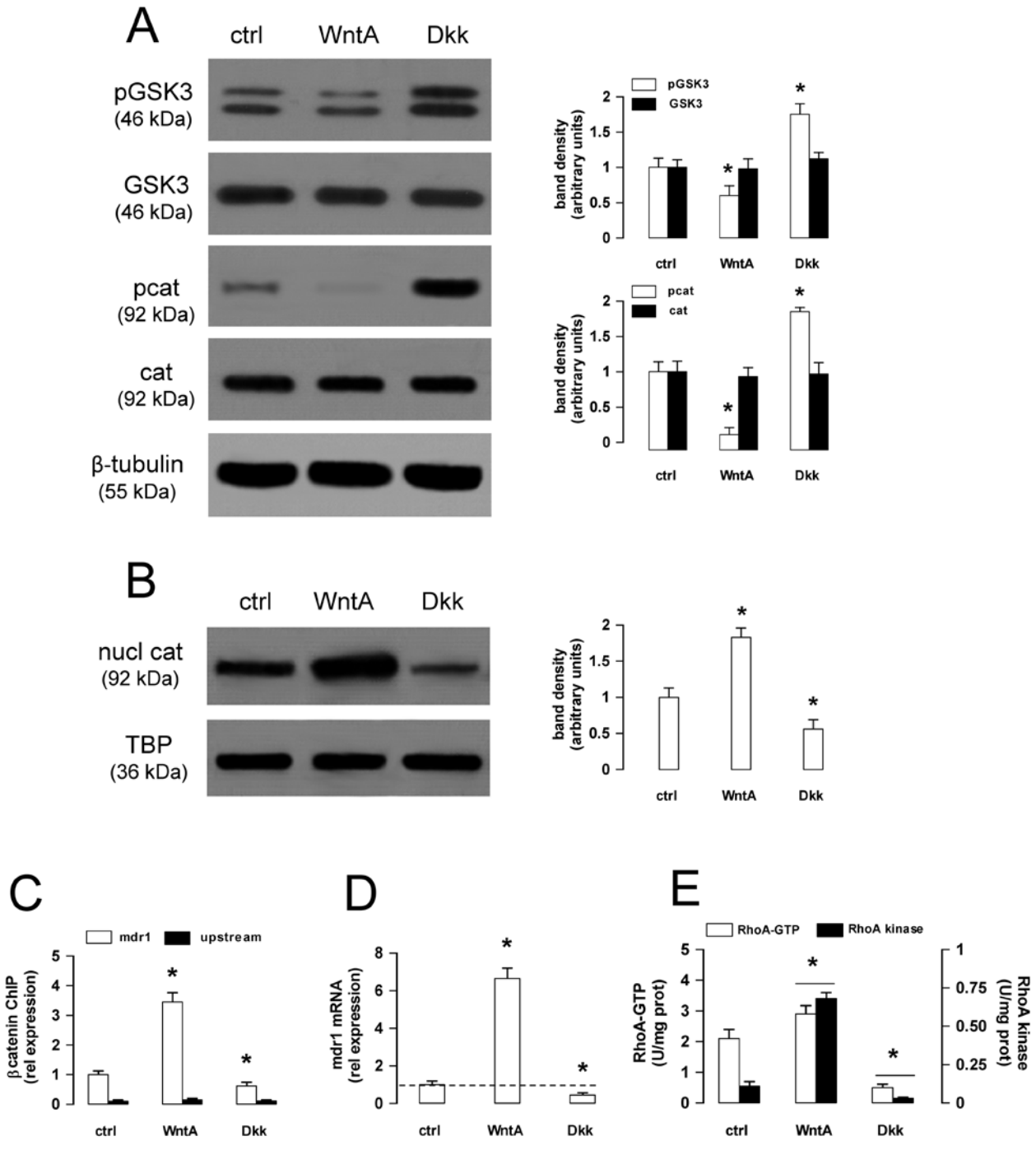
A
ctrl
WntA
Dkk
pGSK3
(46 kDa)
GSK3
(46 kDa)
pcat
(92 kDa)
cat
(92 kDa)
β-tubulin
(55 kDa)
pGSK3
GSK3
band density
(arbitrary units)
pcat
cat
B
nucl cat
(92 kDa)
TBP
(36 kDa)
C
mdr1
upstream
βcatenin ChIP
(rel expression)
D
mdr1 mRNA
(rel expression)
E
RhoA-GTP
RhoA kinase
RhoA-GTP
(U/mg prot)
RhoA kinase
(U/mg prot)

Figure 2

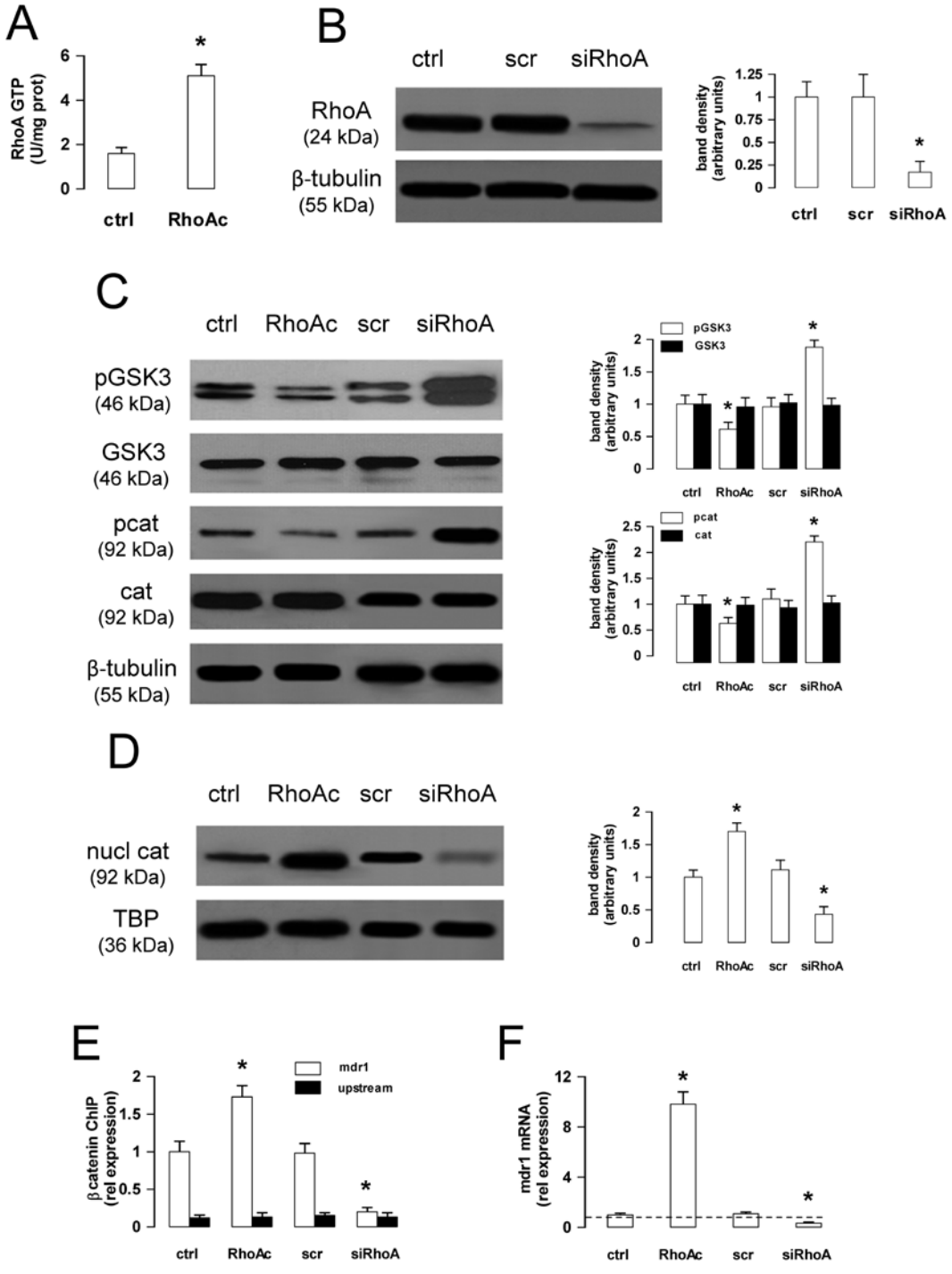
A
RhoA GTP (U/mg prot)
ctrl
RhoAc
B
ctrl
scr
siRhoA
RhoA (24 kDa)
β-tubulin (55 kDa)
band density (arbitrary units)
C
pGSK3 (46 kDa)
GSK3 (46 kDa)
pcat (92 kDa)
cat (92 kDa)
β-tubulin (55 kDa)
D
nucl cat (92 kDa)
TBP (36 kDa)
E
β catenin ChIP (rel expression)
mdr1
upstream
F
mdr1 mRNA (rel expression)

Figure 3

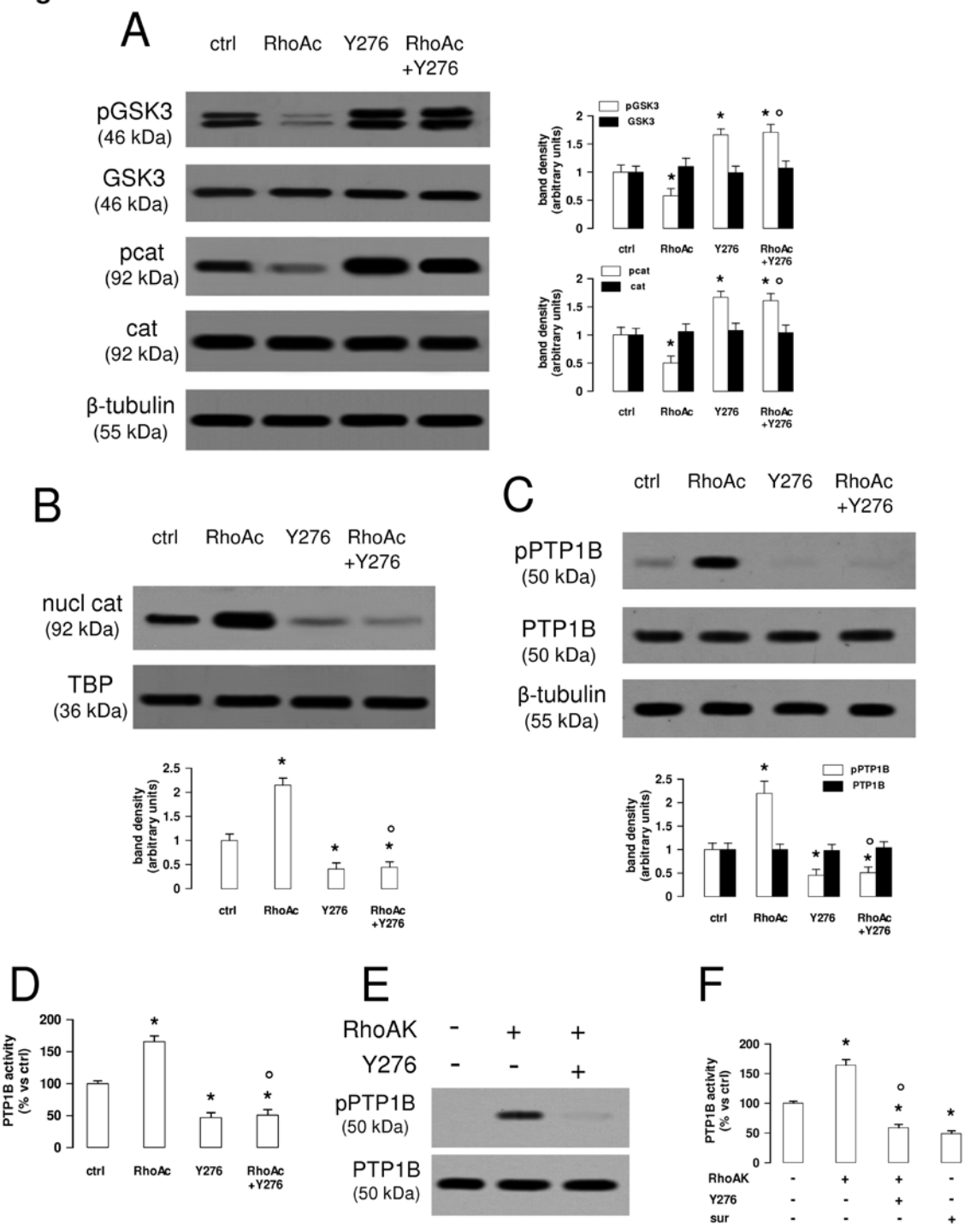
A
ctrl
RhoAc
Y276
RhoAc +Y276
pGSK3 (46 kDa)
GSK3 (46 kDa)
pcat (92 kDa)
cat (92 kDa)
β-tubulin (55 kDa)
band density (arbitrary units)
B
nucl cat (92 kDa)
TBP (36 kDa)
C
pPTP1B (50 kDa)
PTP1B (50 kDa)
β-tubulin (55 kDa)
D
PTP1B activity (% vs ctrl)
E
RhoAK
Y276
pPTP1B (50 kDa)
PTP1B (50 kDa)
F
sur

Figure 4

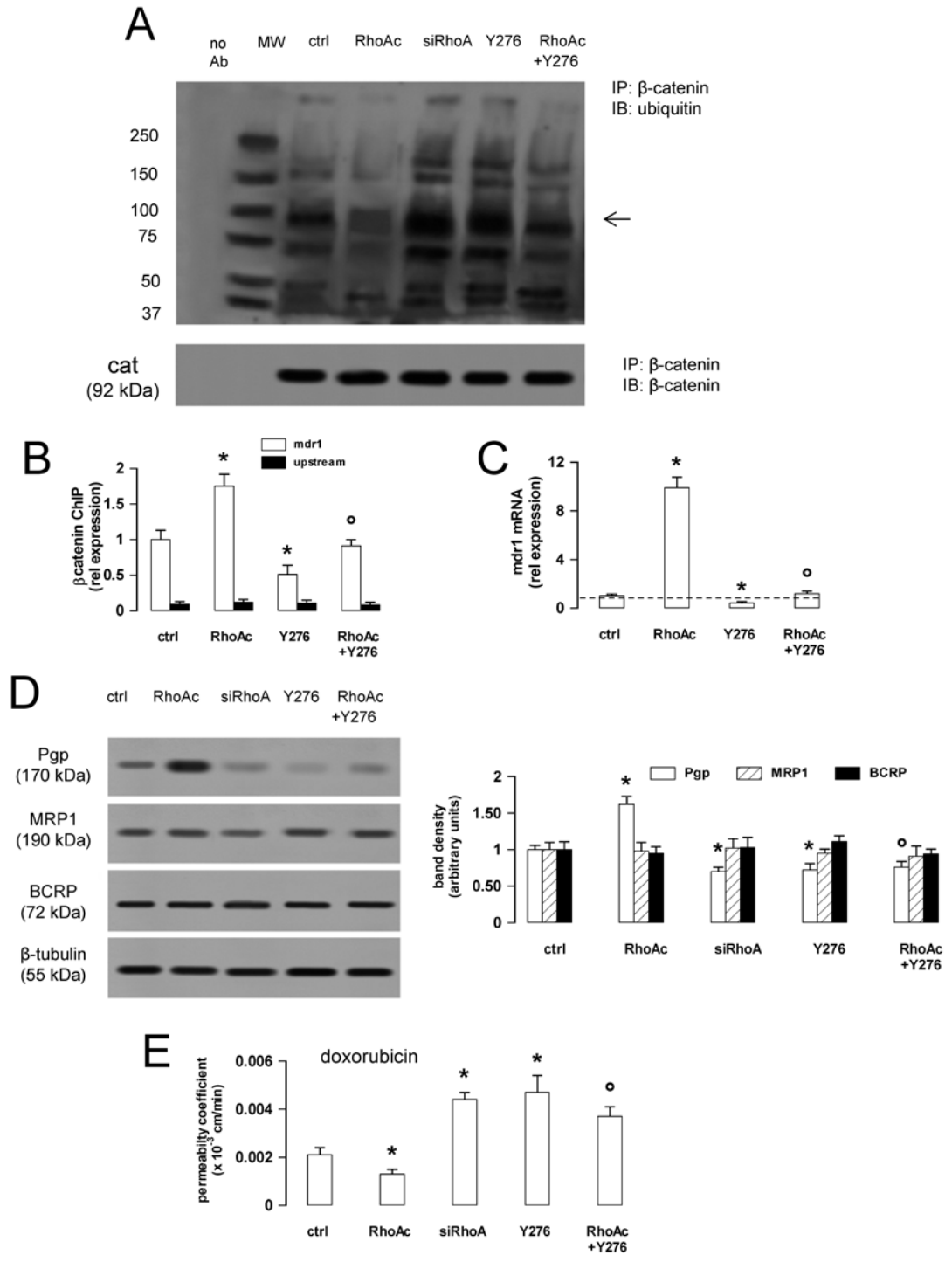
A
no Ab
MW
ctrl
RhoAc
siRhoA
Y276
RhoAc +Y276
IP: β-catenin
IB: ubiquitin
250
150
100
75
50
37
cat (92 kDa)
IP: β-catenin
IB: β-catenin
B
mdr1
upstream
βcatenin ChIP (rel expression)
ctrl
RhoAc
Y276
RhoAc +Y276
C
mdr1 mRNA (rel expression)
D
Pgp (170 kDa)
MRP1 (190 kDa)
BCRP (72 kDa)
β-tubulin (55 kDa)
band density (arbitrary units)
Pgp
MRP1
BCRP
E
doxorubicin
permeability coefficient (x 10-3 cm/min)
siRhoA

Figure 5

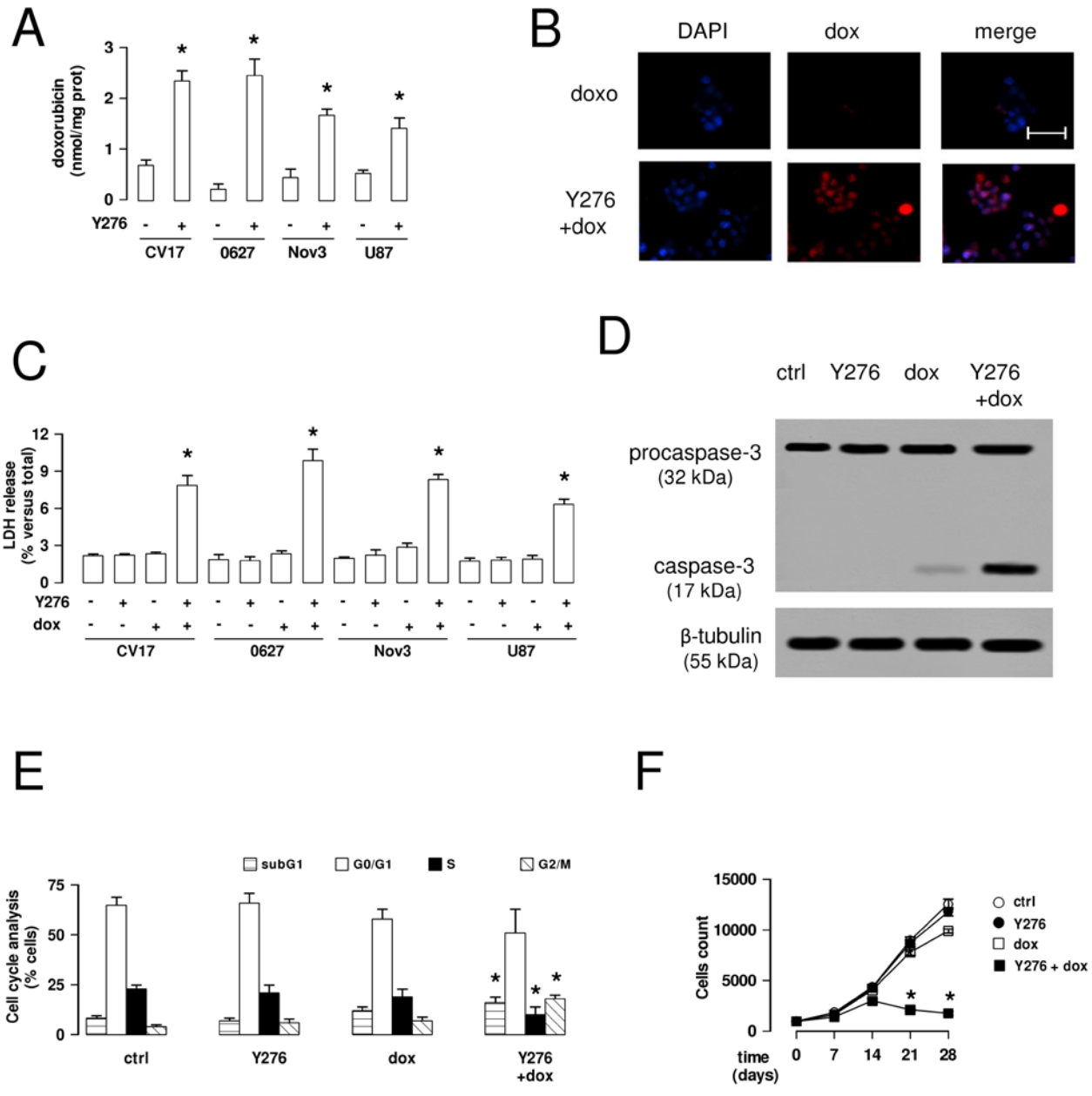
A
doxorubicin (nmol/mg prot)
Y276
CV17
0627
Nov3
U87
B
DAPI
dox
merge
doxo
Y276 +dox
C
LDH release (% versus total)
Y276
dox
CV17
0627
Nov3
U87
D
ctrl
Y276
dox
Y276 +dox
procaspase-3 (32 kDa)
caspase-3 (17 kDa)
β-tubulin (55 kDa)
E
subG1
G0/G1
S
G2/M
Cell cycle analysis (% cells)
ctrl
Y276
dox
Y276 +dox
F
Cells count
time (days)
ctrl
Y276
dox
Y276 + dox

Figure 6

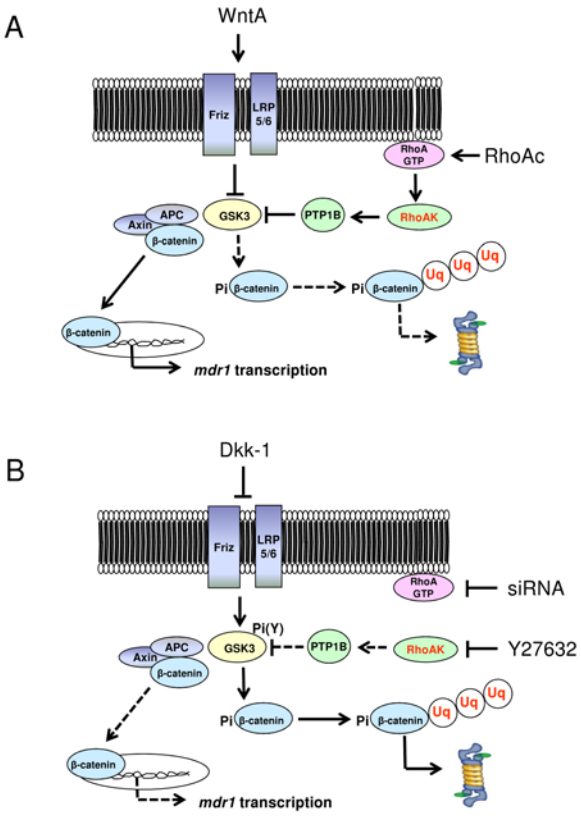
A
WntA
Friz
LRP 5/6
RhoA GTP
RhoAc
APC
Axin
β-catenin
GSK3
PTP1B
RhoAK
Pi
Uq
β-catenin
mdr1 transcription
B
Dkk-1
siRNA
Pi(Y)
Y27632

Supplementary Figures legends

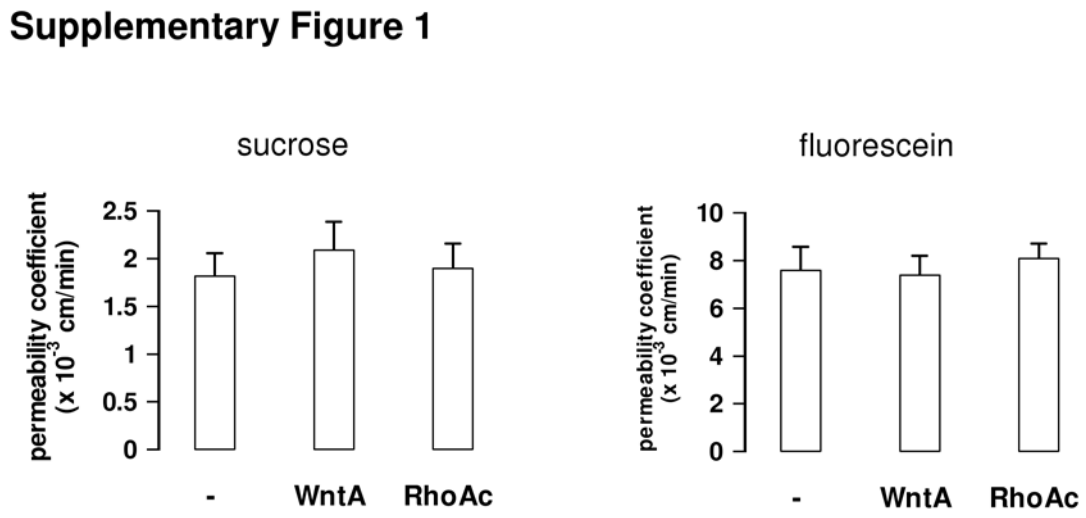

Supplementary Figure 1. Effects of Pgp inducers on the permeability to small molecules in human BBB cells

The hCMEC/D3 cells were grown for 7 days up to confluence in Transwell inserts, then the medium in the upper chamber was replaced with fresh medium (-) or medium containing the Wnt activator 2-amino-4-(3,4-(methylenedioxy)benzylamino)-6-(3-methoxyphenyl)pyrimidine (*WntA*; 20 μmol/L for 24 h) and the RhoA activator II (*RhoAc*; 5 μg/mL for 3 h), chosen as Pgp inducers. At the end of the incubation period, 2 μCi/mL [^{14}C]-sucrose or 10 μg/mL sodium fluorescein were added in the upper chamber. After 3 h the amount of each compound recovered from the lower chamber was measured by liquid scintillation (for sucrose) or fluorimetrically (for sodium fluorescein). Permeability coefficients were calculated as reported under Materials and methods. Measurements were performed in duplicate and data are presented as means $\pm$ SD (n = 3).

Supplementary Figure 2

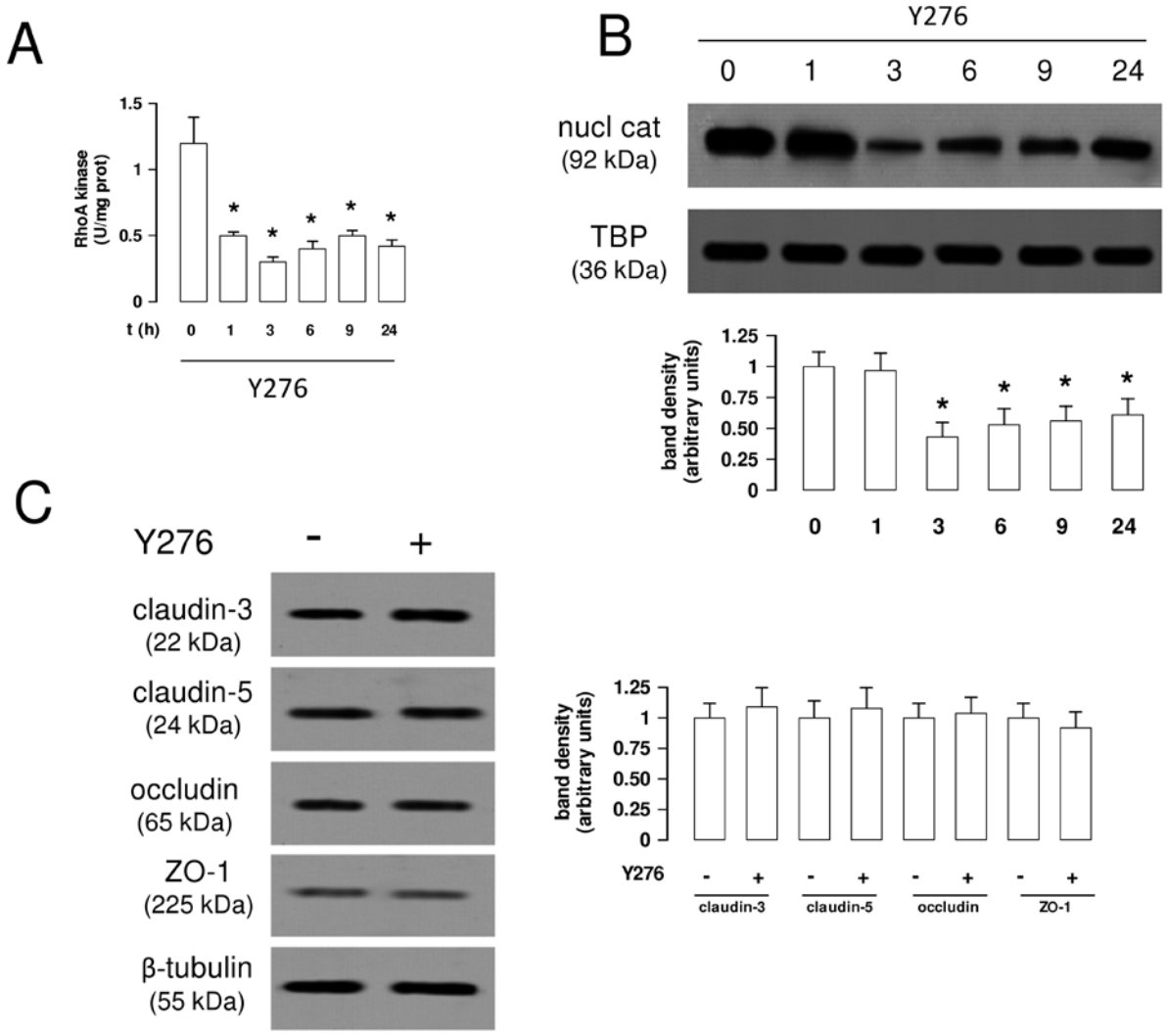

Supplementary Figure 2. The RhoA kinase inhibition decreases the β-catenin translocation in human BBB cells

The hCMEC/D3 cells were cultured in fresh medium in the absence (*0*) or in the presence of 10 μmol/L RhoA kinase inhibitor Y27632 (*Y276*) for 1, 3, 6, 9, 24 h. **A.** RhoA kinase activity. Samples were subjected to ELISA assays to measure the activity of RhoA kinase. Data are presented as means ± SD (n = 4). Versus *ctrl*: * $p < 0.001$. **B.** The nuclear extracts were analyzed for the amount of β-catenin (*nucl cat*). The expression of TBP was used as a control of equal protein loading. The figure is representative of 3 experiments with similar results. The band density ratio between each protein and TBP was expressed as arbitrary units. Versus *ctrl* cells: * $p < 0.01$. **C.** The hCMEC/D3 cells were cultured in fresh medium (-) or in the presence (+) of 10 μmol/L RhoA kinase inhibitor Y27632 (*Y276*) for 3 h, then lysed and subjected to Western blot analysis for claudin-3, claudin-5, occludin, ZO-1. The β-tubulin expression was used as a control of equal protein loading. The figure is representative of 3 experiments with similar results. The band density ratio between each protein and β-tubulin was expressed as arbitrary units. **D.** The hCMEC/D3 cells were grown for 7 days up to confluence in Transwell inserts, then the medium in the upper chamber was replaced with fresh medium (-) or medium containing (+) 10 μmol/L RhoA kinase inhibitor Y27632 (*Y276*) for 3 h. At the end of the incubation period, 2 μmol/L dextran-FITC, 2 μCi/mL [^{14}C]-inulin, or 2 μCi/mL [^{14}C]-sucrose were added in the upper chamber. After 3 h the amount of each compound recovered from the lower chamber was measured fluorimetrically (for dextran-FITC) or by liquid scintillation (for inulin and sucrose). The permeability coefficients were calculated as reported under Materials and methods. Measurements were performed in duplicate and data are presented as means ± SD (n = 3).

Supplementary Figure 3

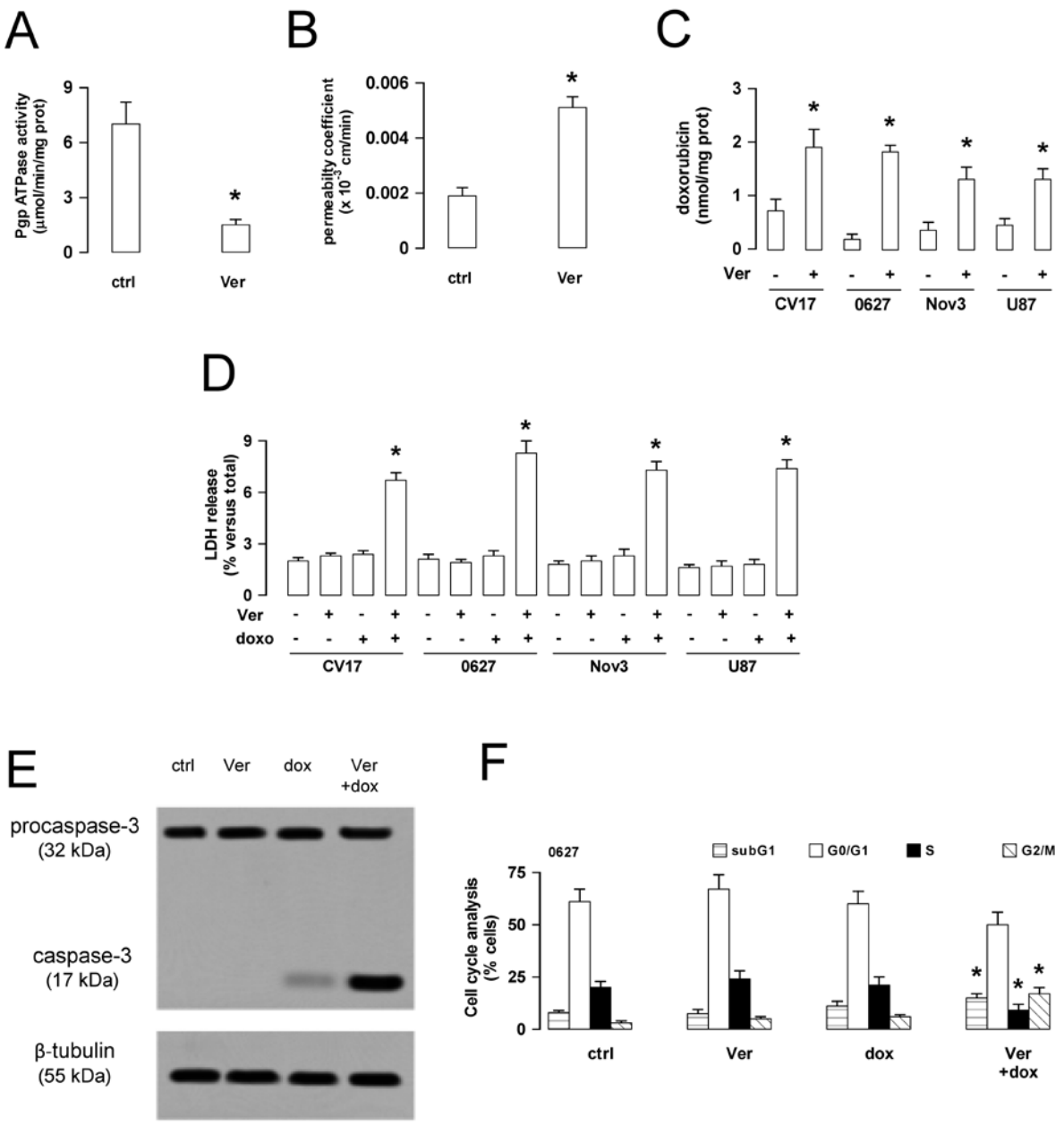

Supplementary Figure 3. Effects of verapamil on doxorubicin permeability and cytotoxicity in glioblastoma cells co-cultured with BBB cells

The hCMEC/D3 cells were grown for 7 days up to confluence in Transwell inserts; the CV17, 01010627, Nov3 and U87-MG cells were seeded at day 4 in the lower chamber. After 3 days of co-culture, the supernatant in the upper chamber was replaced with fresh medium without (- or *ctrl*) or with verapamil (*Ver*; 10 μmol/L) for 3 h (panels **A-C**) or 24 h (panels **D-F**). Doxorubicin (*dox*; 5 μmol/L) was co-incubated in the upper chamber for 3 h (panels **B-C**) or 24 h (panels **D-F**). **A.** The ATPase activity was measured spectrophotometrically after immunoprecipitation of Pgp from membrane fractions. Measurements were performed in duplicate and data are presented as means ± SD (n = 3). Versus *ctrl*: * $p < 0.005$. **B.** The doxorubicin permeability coefficient was calculated as reported under Materials and methods. Measurements were performed in duplicate and data are presented as means ± SD (n = 3). Versus *ctrl*: * $p < 0.001$. **C.** Fluorimetric quantification of intracellular doxorubicin in glioblastoma cells. Data are presented as means ± SD (n = 3). Versus untreated (-) cells: * $p < 0.01$. **D.** Glioblastoma cells were checked spectrophotometrically for the extracellular release of LDH. Data are presented as means ± SD (n= 4). Versus untreated (-) cells: * $p < 0.001$. **E.** The whole cell lysates from 01010627 cells were resolved by SDS-PAGE and immunoblotted with an anti-caspase-3 antibody (recognizing both pro-caspase and cleaved active caspase). The β-tubulin expression was used as a control of equal protein loading. The figure is representative of 3 experiments with similar results. **F.** Cell cycle analysis. The distribution of 01010627 cells in sub-G1, G0/G1, S, G2/M phase was analyzed by flow cytometry, as detailed under Materials and methods. Data are presented as means ± SD (n=4). Vs *ctrl*: * $p < 0.01$.